Conformational Preference and Cis−Trans Isomerization of 4(*R*)-Substituted Proline Residues

Il Keun Song and Young Kee Kang*

Department of Chemistry and Basic Science Research Institute, Chungbuk National University, Cheongju, Chungbuk 361-763, South Korea

Received: August 5, 2005; In Final Form: November 26, 2005

We report here the conformational preference and prolyl cis−trans isomerization of 4(*R*)-substituted proline dipeptides, *N*-acetyl-*N*′-methylamides of 4(*R*)-hydroxy-L-proline and 4(*R*)-fluoro-L-proline (Ac-Hyp-NHMe and Ac-Flp-NHMe, respectively), studied at the HF/6-31+G(d), B3LYP/6-31+G(d), and B3LYP/6-311++G-(d,p) levels of theory. The 4(*R*)-substitution by electron-withdrawing groups did not result in significant changes in backbone torsion angles as well as endocyclic torsion angles of the prolyl ring. However, the small changes in backbone torsion angles ϕ and ψ and the decrease of bond lengths $r(C^{\beta}-C^{\gamma})$ or $r(C^{\gamma}-C^{\delta})$ appear to induce the increase of the relative stability of the trans up-puckered conformation and to alter the relative stabilities of transition states for prolyl cis−trans isomerization. Solvation free energies of local minima and transition states in chloroform and water were calculated using the conductor-like polarizable continuum model at the HF/6-31+G(d) level of theory. The population of trans up-puckered conformations increases in the order Ac-Pro-NHMe < Ac-Hyp-NHMe < Ac-Flp-NHMe in chloroform and water. The increase in population for trans up-puckered conformations in solution is attributed to the increase in population for the polyproline-II-like conformations with up puckering. The barriers $\Delta G_{ct}^{\ddagger}$ to prolyl cis-to-trans isomerization for Ac-Hyp-NHMe and Ac-Flp-NHMe increase as the solvent polarity increases, as seen for Ac-Pro-NHMe. In particular, it was identified that the cis−trans isomerization proceeds through the clockwise rotation about the prolyl peptide bond for Ac-Hyp-NHMe and Ac-Flp-NHMe in chloroform and water, as seen for Ac-Pro-NHMe.

Introduction

Collagen is an abundant fibrous protein of the extracellular matrix in animals. Collagen adopts a supercoiled triple helix, of which each chain consists of the repeating sequence X-Y-Gly, first deduced from X-ray fiber diffraction patterns.[1−4] Each polypeptide chain of the triple helix is in an extended left-handed polyproline II (PPII)-like helix, and the chains are linked by hydrogen bonds between the backbone C═O and N−H groups of X and Gly residues, respectively.[3,4]

In a repeating sequence X-Y-Gly of collagen, X is often Pro and Y is often either Pro or 4(*R*)-hydroxy-L-proline (Hyp). Hyp residues at the Y position are due to the posttranslational modification of Pro residues by the enzyme prolyl-4-hydroxy-lase. From NMR[5] and recent high-resolution X-ray diffraction[6−8] studies on $(Pro\text{-}Hyp\text{-}Gly)_{10}$ and $(Pro\text{-}Pro\text{-}Gly)_{10}$ peptides as models of the collagen triple helix, it was found that prolyl rings at the X position prefer the down (or C^{γ}-endo) puckering, whereas the up (or C^{γ}-exo) puckering is favored for those at the Y position. The down- and up-puckered conformations are defined as those of which the C^{γ} atom and the C═O group of the Pro residue lie on the same and opposite sides, respectively, of the plane defined by three atoms C^{δ}, N, and C^{α} (Figure 1).[9]

The presence of Hyp residues at the Y position has led to an increase in the thermal stability of collagen[10] and the peptide $(Pro\text{-}Hyp\text{-}Gly)_{10}$.[11−13] The hydroxy groups of Hyp residues have been recognized to play a role in the formation of hydrogen bonding networks with water molecules, which link adjacent chains and consequently stabilize the triple helix.[6,14−16]

* Author to whom correspondence should be addressed. Phone: +82-43-261-2285. Fax: +82-43-273-8328. E-mail: ykkang@chungbuk.ac.kr.

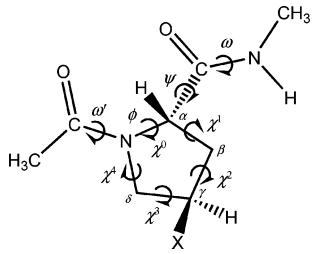

Figure 1. Definition of torsion angles and structural parameters for the Hyp and Flp residues: X = OH for Hyp; X = F for Flp.

From thermal denaturation studies of collagen mimics $(Pro\text{-}Y\text{-}Gly)_{10}$, where Y is Pro, Hyp, and 4(*R*)-fluoro-L-proline (Flp), it was reported that the thermal stability of the triple helix increases in the order $(Pro\text{-}Pro\text{-}Gly)_{10}$ < $(Pro\text{-}Hyp\text{-}Gly)_{10}$ < $(Pro\text{-}Flp\text{-}Gly)_{10}$.[12,13] It was suggested that the substitution at the 4(*R*) position of the prolyl ring by electron-withdrawing groups such as OH and F can stabilize the triple helix of collagen, because the neutral F group has a low propensity to form hydrogen bonds. Upon the basis of the X-ray structure of *N*-acetyl-4(*R*)-fluoro-L-proline methyl ester (Ac-Flp-OMe),[17] the favorable interaction between the carbonyl oxygen preceding the prolyl residue and the carbonyl carbon of the prolyl residue was proposed to stabilize both the trans prolyl peptide bond and the backbone ψ value that is appropriate for the triple helix formation.[18] The increase in the population of the trans conformers for Ac-Flp-OMe versus Ac-Pro-OMe was interpreted as the $n \rightarrow \pi^*$ interaction between these two carbonyl groups by the natural bond orbital (NBO) analysis.[19] The higher trans populations of proline residues versus noncyclic tertiary amides were also described by this $n \rightarrow \pi^*$ interaction.[20] The

10.1021/jp054351h CCC: $33.50
Published on Web 01/05/2006

preference of up puckering for the Flp residue was explained in terms of the gauche effect in the F−C$^{\gamma}$−C$^{\delta}$−N torsion, resulting in the maximum number of gauche interactions between adjacent polar bonds.[13,19] This was ascribed to the favored interactions between the C$^{\gamma}$−F σ* antibonding orbital and the vicinal C−H σ bonding orbital by NBO analyses.[19,21]

However, these two models described by the water-mediated hydrogen bonds and the inductive effects cannot satisfactorily explain the instability of the (Hyp-Pro-Gly)$_{10}$ triple helix[22] as well as either (hyp-Pro-Gly)$_{10}$ or (Pro-hyp-Gly)$_{10}$ triple helices,[23] where hyp is 4(*S*)-hydroxy-L-proline. Upon the basis of the correlation between prolyl puckering and backbone torsion angles observed for X-ray structures of the (Pro-Pro-Gly)$_{10}$ triple helix[24] and proteins,[25] it was suggested that the intrinsic conformational propensities of prolyl residues may play a crucial role in determining both stereospecificity and positional preference and in stabilizing proline-rich collagen polypeptides. However, this proposal cannot be also applied to explain the thermal instability of the (hyp-Pro-Gly)$_{10}$[23] triple helix as well as the thermal stability of the (flp-Pro-Gly)$_{10}$[26,27] triple helix.

Recently, from differential scanning calorimetry analyses of a series of collagen model peptides, it was suggested that the enthalpy term is primarily responsible for the enhanced stability of the triple helix of (Pro-Hyp-Gly)$_{10}$, whereas the entropy term dominates the enhanced stability of (Pro-Flp-Gly)$_{10}$.[28] In addition, by comparison of the molecular volumes observed in solution and the intrinsic molecular volumes calculated from crystal structures, it was proposed that (Pro-Hyp-Gly)$_{10}$ is more hydrated compared to (Pro-Flp-Gly)$_{10}$, which contributes to the larger enthalpy.[28] In particular, it has been reported that two peptides, (Hyp-Hyp-Gly)$_{10}$[29] and Ac-(Gly-Hyp-Hyp)$_{10}$-NH$_2$,[30] form stable triple helices, and the puckering of the Y-position Hyp in the X-ray structure of (Hyp-Hyp-Gly)$_9$ is up-puckered.[31]

The 4(*R*)-substitution of electron-withdrawing groups such as OH and F at the C$^{\gamma}$ atom of the prolyl ring has resulted in substantial effects on the chemical properties of Ac-Pro-OMe.[32] With the increase in the electron-withdrawing effect, the pK_a of the prolyl nitrogen and the amide I frequency of the C═O stretching decreased. In addition, the conformers with the trans prolyl peptide bond more were populated with the more electronegative substituent.[18,32] However, there are no remarkable differences in rotational barriers of prolyl cis-to-trans and trans-to-cis isomerizations of Ac-Pro-OMe, Ac-Hyp-OMe, and Ac-Flp-OMe in water.[32,33] In particular, the presence of electron-withdrawing substituents has significantly affected the prolyl puckering, as mentioned above. In crystal[17] and solution,[19,32] Ac-Hyp-OMe and Ac-Flp-OMe strongly prefer the up puckering, whereas the unsubstituted Ac-Pro-OMe adopts both up and down puckerings.

Considerable ab initio computations on the proline residue have been reported at various levels of theory.[34,35] However, there are a limited number of ab initio calculations carried out on Hyp,[21,36−39] Flp,[19,21,37,39] hyp,[21] and 4(*S*)-fluoro-L-proline (flp)[19,21] residues at Hartree−Fock (HF), Møller−Plesset perturbation (MP2), and/or density functional theory (DFT) levels of theory to date. Some ab initio calculations[19,21,36,39] confirmed the experimental finding that the trans up-puckered conformations of the Hyp and Flp residues are preferred in crystal[17] and solution.[18,32] Some ab initio computations[21,39] are also consistent with the observed increase of trans conformations in solution as the electron-withdrawing ability of the 4(*R*)-substituent increases.[18,32] Rankin and Boyd identified the transition states for the prolyl cis−trans isomerization of Hyp and Flp dipeptides and proposed that this isomerization may proceed through the counterclockwise rotation of the prolyl peptide bond with the torsion angle $\omega' \approx -90°$ (Figure 1).[37] Lam et al. located 20 local minima of the Hyp dipeptide at the B3LYP/6-31G(d) level of theory after taking the orientation of the side chain OH group into account.[38] At the HF/6-31+G(d) and B3LYP/6-311++G-(d,p) levels of theory, we recently identified that the puckering transition of the prolyl ring for the Hyp and Flp residues proceeds from a down-puckered conformation to an up-puckered one through the transition state with an envelope form having the N atom at the top of envelope rather than a planar one for both trans and cis conformers,[40] which is the same as found for the unsubstituted proline residue.[41] However, the 4(*R*)-substitution by hydroxy and fluorine groups has brought some structural changes in the prolyl ring of the transition states and changes in barriers for the puckering transition.

Although most of the previous ab initio studies have mainly focused on the conformational preference of Hyp and Flp residues in understanding the stability of the collagen triple helix, only representative conformations were considered to explain the preference of trans up-puckered conformations in the gas phase and in water. However, all feasible conformations should be taken into account to explain reasonably the observed conformational preference. In particular, the change in rotational barriers for the prolyl cis−trans isomerization by electron-withdrawing substituents at the C$^{\gamma}$ atom of the Pro residue in solution has never been quantum-mechanically studied, although the change for the Pro, Hyp, and Flp residues was reported to be insignificant from NMR experiments in water.[32,33] In addition, the change in the rotational barriers for the Hyp and Flp residues with the increase of solvent polarity has never been extensively investigated, whereas the solvent polarity has been known to affect largely the prolyl rotational barrier of the Pro residue.[34,35,42]

We report here the results on 4(*R*)-substituted proline (Hyp and Flp) dipeptides calculated using ab initio HF and DFT methods with the self-consistent reaction field (SCRF) method to determine the effects of the 4(*R*)-substitution of the prolyl ring by electron-withdrawing groups on the conformational preference and prolyl cis−trans isomerization in the gas phase, chloroform, and water. In particular, the conformational preference was analyzed utilizing all feasible conformations found from the survey of the backbone potential energy surface (PES) and from the search of local minima and transition states for both Hyp and Flp dipeptides.

Computational Methods

Chemical structures and torsional parameters for the backbone and prolyl ring of the Hyp and Flp residues are defined in Figure 1. All ab initio and density functional calculations were carried out using the Gaussian 98[43] and Gaussian 03[44] packages. The values of the backbone torsion angles ϕ and ψ for local minima of Ac-Pro-NHMe optimized at the HF/6-31+G(d) level[34] were used as starting points for the empirical energy optimization of Ac-Hyp-NHMe using the ECEPP/3 force field[45] that has been used for the conformational study of Pro- or Hyp-containing peptides. These minimized conformations from empirical energy calculations were used as initial structures for the optimization of Ac-Hyp-NHMe at the HF/6-31+G(d) level of theory. For each initial structure of Ac-Hyp-NHMe, three orientations, i.e., gauche+, gauche−, and trans, of the OH group were taken into account, which were defined by the C$^{\beta}$−C$^{\gamma}$−O$^{\delta 1}$−H torsion angle. The optimization of each local minimum for Ac-Flp-NHMe at the HF/6-31+G(d) level of theory was started from that of Ac-Pro-NHMe,[34] in which the 4(*R*)-H atom of the Pro residue was replaced by an F atom.

Here, each backbone conformation of Ac-Hyp-NHMe and Ac-Flp-NHMe is represented by a capital letter depending on its values of ϕ and ψ for the backbone.[46] Conformations C, A, and F are defined by the backbone torsion angle ψ with the backbone torsion angle ϕ in the range of $-110° < \phi < -40°$: conformation C, $50° < \psi < 130°$; conformation A, $-90° < \psi < -10°$; conformation F, $130° < \psi < 180°$ or $-180° < \psi < -140°$. Conformations C, A, and F correspond to the γ-turn, α-helical, and polyproline-like structures, respectively. Trans and cis conformations for the Ac−Hyp and Ac−Flp peptide bonds are defined by the orientation of the methyl carbon of the acetyl group and the C^{α} of the Pro residue, which are denoted by "t" and "c", respectively. Down- and up-puckered conformations are defined as those of which the C^{γ} atom and the C═O group of the prolyl residue lie on the same and opposite sides, respectively, of the plane defined by three atoms C^{δ}, N, and C^{α} (Figure 1), which are represented by "d" and "u", respectively. In addition, the orientations of the hydroxy group of the Hyp residue are denoted by t, g^+, and g^- for trans, gauche+, and gauche−, respectively. For example, the letter code $tCdg^-$ of Ac-Hyp-NHMe is the down-puckered conformation C with the trans prolyl peptide bond and the gauche− hydroxy orientation.

Because the two polyproline-like conformations tFd and tFu were found not to be local minima for both Ac-Hyp-NHMe and Ac-Flp-NHMe in the gas phase but to be feasible in water (see Figures 2 and 3 for the conformational energy profiles along the ψ angle at the HF/6-31+G(d) level of theory), they were located by adiabatic optimizations with the ψ values fixed at those optimized for Ac-Hyp-NMe_2 and Ac-Flp-NMe_2 at the HF/6-31+G(d) level of theory, as done for Ac-Pro-NHMe.[34] In addition, the conformation tAd was the same case and obtained by adiabatically optimizing at the ψ value of the conformation cAd for each of Ac-Hyp-NHMe and Ac-Flp-NHMe. At the HF/6-31+G(d) level of theory, the transition states ts1 and ts2 were located by optimizing the conformations obtained from the adiabatic optimization of the conformations cAd and cAu, respectively, with $\omega' = +116°$ for Ac−Hyp and Ac−Flp bonds (Figure 1), as done for Ac-Pro-NHMe.[34] The transition states ts3 and ts4 were located starting from the ts1 and ts2 with $\omega' = -65°$, respectively.

Local minima and transition states optimized at the HF/6-31+G(d) level were used as initial points for optimizations at hybrid density functional B3LYP/6-31+G(d) and B3LYP/6-311++G(d,p) levels of theory. As done at the HF/6-31+G(d) level, conformations tFd, tFu, and tAd were located by adiabatic optimizations at both B3LYP levels. In addition, the conformation tAu is no longer a local minimum for Ac-Hyp-NHMe and Ac-Flp-NHMe at these two B3LYP levels and is located by adiabatically optimizing at the ψ value of the conformation cAd for each of Ac-Hyp-NHMe and Ac-Flp-NHMe. Vibrational frequencies were calculated for all stationary points at HF and B3LYP levels of theory, which were used to compute enthalpies and Gibbs free energies with scale factors of 0.89[47] and 0.98[47,48] at HF and B3LYP levels of theory, respectively, at 25 °C and 1 atm. Scale factors of 0.89 and 0.98 at HF/6-31+G(d) and B3LYP/6-31+G(d) levels of theory, respectively, were chosen to reproduce experimental frequencies for the amide I band of *N*-methylacetamide in Ar and N_2 matrixes.[47] A scale factor of 0.98 at the B3LYP/6-311++G(d,p) level of theory reproduced well some experimental frequencies of proline in an Ar matrix.[48] Each transition state was confirmed by checking whether it has one imaginary frequency after frequency calculations at the HF and B3LYP levels of theory. In a recent work on proline, the B3LYP/6-311++G(d,p) level of theroy provided the relative energies very close to those obtained at the extrapolated CBS CCSD(T) level of theory, and the rotational constants are in good agreement with those determined experimentally.[49] In addition, the B3LYP/6-311++G(d,p) level of theory was reported to be quite effective in giving satisfactory calculated geometries for a series of organic molecules, compared to the CCSD and MP2 levels with 6-311++G(d,p) and aug-cc-pVDZ basis sets.[50]

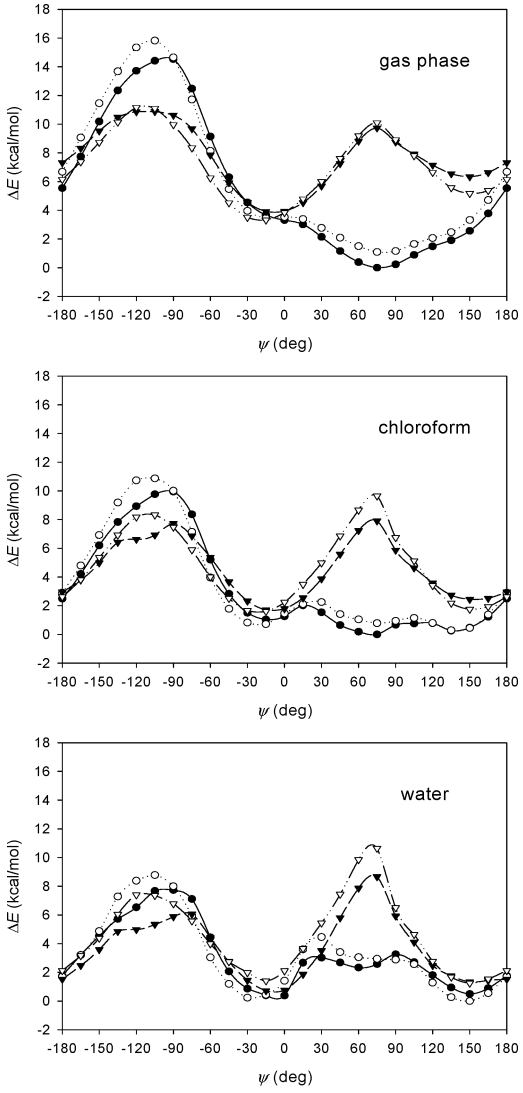

Figure 2. Potential energy surfaces of Ac-Hyp-NHMe at the HF/6-31+G(d) level of theory with the CPCM-UAHF(G98) method along the backbone torsion angle ψ in the gas phase, chloroform, and water: trans-down, ●; trans-up, ○; cis-down, ▼; cis-up, ▽.

The two-dimensional potential energy surfaces (PESs) of the down- and up-puckered conformations with trans and cis peptide bonds for Ac-Hyp-NHMe and Ac-Flp-NHMe were calculated along the backbone torsion angle ψ at the HF/6-31+G(d) level of theory, in which adiabatic optimizations were performed at each value of ψ with an interval of 15° for $-180° \le \psi \le 180°$. The local minima $tCdg^-$, $tCug^-$, $cAdg^-$, and $cAug^-$ for Ac-Hyp-NHMe (Table 1) and the local minima tCd, tCu, cAd, and cAu for Ac-Flp-NHMe (Table 2) were used as initial structures for adiabatic optimizations.

We employed the conductor-like polarizable continuum model (CPCM) SCRF method,[51] implemented in the Gaussian 98[43] and Gaussian 03[44] packages, to compute solvation free energies (ΔG_s) at the HF/6-31+G(d) level of theory with UAHF and

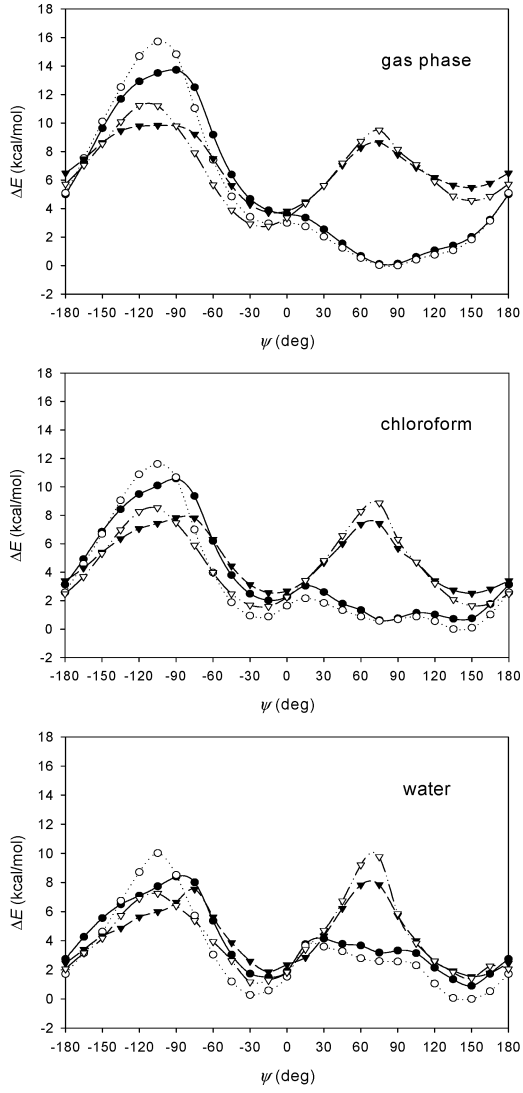

Figure 3. Potential energy surfaces of Ac-Flp-NHMe at the HF/6-31+G(d) level of theory with the CPCM-UAHF(G98) method along the backbone torsion angle ψ in the gas phase, chloroform, and water: trans-down, ●; trans-up, ○; cis-down, ▼; cis-up, ▽.

UAKS cavities, which are the united atom topological model (UATM) radii optimized for HF/6-31G(d) and density functional PBE0/6-31G(d) levels of theory, respectively.[52] In this work, the CPCM-UAHF method of Gaussian 98 and the CPCM-UAKS method of Gaussian 03 are represented by CPCM-UAHF(G98) and CPCM-UAKS(G03), respectively. For CPCM-UAHF(G98) and CPCM-UAKS(G03) calculations, the default average areas of 0.4 and 0.2 Å^2 for tesserae were used, respectively. Solvation free energies of Ac-Hyp-NHMe and Ac-Flp-NHMe were calculated for their local minima and transition states optimized at HF and B3LYP levels of theory and PESs optimized at the HF/6-31+G(d) level of theory in the gas phase. The solvents considered here are nonpolar chloroform and polar water, whose dielectric constants are 4.9 and 78.4 at 25 °C, respectively. We calculated two kinds of relative total free energies to interpret the conformational preferences in solution: (a) the relative total free energy $\Delta G_{tot}{}^0$ computed by the sum of the relative electronic energy (ΔE_e) and the relative solvation free energy ($\Delta\Delta G_s$) and (b) the relative total free energy ΔG_{tot} computed by the sum of the relative Gibbs free energy (ΔG) and $\Delta\Delta G_s$. Here, $\Delta\Delta G_s$ is the solvation free energy relative to the lowest-energy conformation with $\Delta E_e = 0.00$ kcal/mol. Recently, relative total free energies $\Delta G_{tot}{}^0$ calculated using the CPCM-UAHF(G98) method at the HF/6-31+G(d) level of theory predicted well the experimental populations of backbone and cis conformations for Ac-Pro-NHMe[34] and Ac-Pro-NMe$_2$[35] as well as the experimental rotational barriers about the C−N bond of amides[53] in chloroform and water. In addition, the CPCM-UAKS(G03) calculations for a number of neutral and charged organic molecules at the HF/6-31+G(d)//HF/6-31+G(d) and HF/6-31+G(d)//B3LYP/6-31+G(d) levels of theory provided hydration free energies in agreement with available experimental data.[54]

Results and Discussion

Conformations in the Gas Phase. The two-dimensional potential energy surfaces (PESs) of Ac-Hyp-NHMe and Ac-Flp-NHMe with trans/cis peptide bonds and down/up puckerings were calculated along the backbone torsion angle ψ at the HF/6-31+G(d) level of theory, as shown in Figures 2 and 3, respectively. Although the overall shapes of PESs for Ac-Hyp-NHMe and Ac-Flp-NHMe are quite similar to those of Ac-Pro-NHMe in ref 34, the relative stabilities of conformations and the barriers for conformational transitions are different from each other, as described below.

For Ac-*trans*-Hyp-NHMe, the PESs at the HF/6-31+G(d) level of theory show one minimum tCdg$^-$ at $\psi = 77°$ for the down-puckered conformation and two minima tAug$^-$ and tCug$^-$ at $\psi = -11°$ and 81°, respectively, for the up-puckered conformation (Table 1). First two lowest-energy conformations tCdg$^-$ and tCug$^-$ have a common C_7 hydrogen bond between C═O of the N-terminal group and N−H of the C-terminal group, which is known to be responsible for stabilizing the lowest-energy conformations of proline dipeptides[34,41,42,55,56] and dipeptides of proline derivatives such as pseudo-prolines[57] and 5-methylated prolines.[58] This C_7 hydrogen bond appears to cause the PPII-like conformations tFd and tFu to be inaccessible. Our PESs for Ac-*trans*-Hyp-NHMe with down and up puckerings are found to be similar to those of Benzi et al. obtained at the HF/6-31G(d) level of theory,[36] except the difference in relative stabilities of conformations tCdg$^-$ and tCug$^-$. The barriers for conformational transitions of tAu → tCu for Ac-Hyp-NHMe at $\psi = 0°$ and $-105°$ are estimated to be 0.1 and 12.4 kcal/mol, respectively, whereas the corresponding values for Ac-Pro-NHMe are 0.3 and 11.9 kcal/mol, respectively. However, the corresponding barriers for down-puckered conformations cannot be estimated because the conformation tAd is not a local minimum.

For the PESs of Ac-*cis*-Hyp-NHMe at the HF/6-31+G(d) level of theory, there are two minima cAdg$^-$ and cFdg$^-$ at $\psi = -8°$ and 149°, respectively, for the down-puckered conformation and two minima cAug$^-$ and cFug$^-$ at $\psi = -20°$ and 149°, respectively, for the up-puckered conformation (Table 1). In particular, the higher barriers appear at $\psi = 75°$ for the backbone conformation C, which may be ascribed by the unfavorable nonbonded interaction between the methyl carbon of acetyl group and the C$^\alpha$ of the Hyp residue and by the weak electrostatic interaction between the carbonyl oxygen of the acetyl group and the carbonyl carbon of the Hyp residue, as seen for Ac-*cis*-Pro-NHMe.[34,55,59] The lack of the C_7 hydrogen bond between two terminal groups seems to allow the polyproline I (PPI)-like conformations cFd and cFu to be feasible. Although the overall shapes of the PESs of Ac-*cis*-Hyp-NHMe are similar to those of Ac-*cis*-Pro-NHMe (ref 34), the barriers for transitions cA → cF at $\psi = -120°$ and 75° for down- and up-puckered structures of Ac-Hyp-NHMe are almost identical, which are lower by about 2−3 kcal/mol than those of Ac-Pro-

TABLE 1: Backbone Torsion Angles, Endocyclic Torsion Angles, and Puckering Amplitudes of Ac-Hyp-NHMe Optimized at the HF/6-31+G(d) Level of Theory in the Gas Phase

	backbone torsion angles[a]				endocyclic torsion angles[a]						puckering amplitude	thermodynamic quantities		
conformer[b]	ω'	ϕ	ψ	ω	χ^0	χ^1	χ^2	$\chi^{3,1}$	χ^4	$\chi^{3,2}$	q_z[c]	ΔE_e[d]	ΔH[e]	ΔG[f]
tCdg$^-$	−172.7	−86.1	77.3	−175.9	−14.0	31.9	−38.2	29.4	−9.7	−78.6	0.372	0.00	0.00	0.00
tCug$^-$	−170.4	−86.8	80.7	−174.7	−8.2	−16.1	33.3	−37.7	29.2	−62.3	0.369	1.05	1.10	1.24
tCdg$^+$	−173.7	−85.5	78.4	−175.7	−14.0	31.3	−37.2	28.3	−9.0	49.6	0.362	1.68	1.64	1.61
tCut	−172.0	−85.0	84.0	−174.5	−8.1	−16.2	33.1	−37.4	28.8	−173.2	0.366	1.86	1.88	1.96
tFdg$^-$ [g]	179.0	−70.1	136.1	−176.1	−12.0	29.3	−36.0	28.3	−10.3	−82.7	0.351	1.95	1.84	1.13
tCug$^+$	−175.8	−83.0	83.7	−174.5	−12.4	−12.9	32.0	−38.8	32.6	48.3	0.378	2.19	2.21	2.15
tFdt[g]	178.5	−70.0	138.2	−176.4	−12.7	29.9	−36.0	27.9	−9.5	−156.9	0.351	2.28	2.14	1.40
tFug$^-$ [g]	−178.8	−64.5	134.8	−175.1	1.4	−23.3	35.9	−34.4	21.1	−66.0	0.362	2.47	2.32	1.93
tFut[g]	179.6	−62.9	136.1	−175.4	0.3	−22.7	35.8	−35.0	22.0	−178.3	0.364	2.74	2.57	2.18
tFug$^+$ [g]	173.8	−61.0	139.1	−176.1	−10.4	−15.1	33.6	−38.9	31.5	62.5	0.383	2.96	2.82	2.40
tFdg$^+$ [g]	177.3	−69.2	139.7	−176.6	−13.8	30.0	−35.3	26.6	−8.0	55.0	0.346	3.17	3.04	2.51
cAut	9.9	−82.3	−19.1	−178.1	0.9	−24.0	37.4	−36.5	22.5	174.9	0.380	3.30	3.08	2.63
tAug$^-$	−167.6	−79.6	−11.4	174.7	2.6	−24.9	37.2	−35.4	20.8	−60.8	0.374	3.45	3.27	2.95
tAdg$^-$ [h]	−169.2	−85.1	−7.9	173.5	−9.3	29.5	−38.7	32.6	−14.7	−72.4	0.378	3.46	3.24	2.65
cAdg$^-$	9.1	−89.6	−7.9	180.0	−13.0	31.2	−38.0	29.8	−10.5	−74.7	0.371	3.86	3.64	3.17
cAug$^-$	7.2	−79.1	−19.9	−177.8	3.6	−25.7	37.6	−35.0	19.9	−67.5	0.375	3.87	3.63	3.21
cAdt	9.3	−88.1	−10.9	179.8	−11.1	29.9	−37.5	30.4	−12.1	−169.9	0.366	4.03	3.80	3.28
tAdt[h]	−169.2	−83.7	−10.9	173.6	−7.4	28.2	−38.2	33.3	−16.2	−160.4	0.375	4.33	4.07	3.45
cAdg$^+$	9.7	−88.9	−10.2	−179.5	−12.5	30.6	−37.5	29.7	−10.8	58.6	0.367	4.47	4.26	3.82
tAut	−168.8	−77.3	−13.6	174.8	3.0	−25.1	37.1	−34.9	20.1	−174.3	0.371	4.59	4.36	4.04
tAdg$^+$ [h]	−170.0	−83.7	−10.2	174.1	−7.9	28.4	−38.1	32.8	−15.7	48.3	0.374	4.60	4.36	3.85
tAug$^+$	−171.5	−77.7	−13.9	175.4	−0.8	−22.7	36.8	−36.8	23.8	44.6	0.378	4.78	4.56	4.05
cAug$^+$	2.7	−75.2	−21.6	−177.4	−3.1	−20.5	35.6	−36.8	25.4	72.5	0.372	5.09	4.80	3.95
cFut	1.3	−61.7	152.1	175.7	4.1	−26.1	37.7	−34.8	19.4	171.9	0.376	5.17	4.89	3.99
cFdt	−0.5	−73.6	152.3	175.1	−14.6	31.5	−36.9	27.8	−8.2	−169.2	0.362	5.81	5.53	4.29
cFdg$^-$	0.4	−74.5	148.9	176.1	−14.2	31.1	−36.7	27.9	−8.6	−86.6	0.360	6.34	6.04	4.71
cFug$^+$	−7.7	−58.8	156.6	174.9	−6.7	−18.5	35.6	−38.9	29.1	83.7	0.387	6.44	6.13	4.96
cFug$^-$	0.1	−59.4	149.0	177.2	6.7	−27.4	37.6	−33.2	16.8	−73.3	0.371	6.51	6.20	5.39
cFdg$^+$	−0.9	−74.5	153.7	175.2	−17.0	32.3	−36.2	25.8	−5.5	65.8	0.358	6.84	6.54	5.32
ts2	120.4	−108.6	−10.3	−177.4	3.6	−26.5	38.3	−36.7	20.9	73.2	0.388	16.95	15.96	17.07
ts4	−69.1	−85.7	−6.7	177.8	17.5	−34.8	38.7	−28.3	6.8	−64.7	0.384	18.70	17.59	17.87
ts1	115.5	−106.6	−8.0	−178.8	4.3	21.2	−37.9	40.6	−28.2	−71.3	0.403	18.89	17.77	18.16
ts3	−65.4	−94.3	1.5	176.7	3.8	20.8	−36.8	38.7	−26.9	−74.3	0.388	20.06	18.89	18.46

[a] Defined in Figure 1; units in degrees. [b] See the text for definition. For example, the first letter code tCdg$^-$ is the down-puckered conformation C with the trans prolyl peptide bond and the gauche− hydroxy orientation. [c] Units in angstroms; the puckering amplitude q_z corresponds to the maximum *z*-displacement perpendicular to the mean plane of the ring, defined by Cremer and Pople in ref 60. [d] Relative electronic energies in kcal/mol. [e] Relative enthalpy changes in kcal/mol at 25 °C. [f] Relative Gibbs free energy changes in kcal/mol at 25 °C. [g] Optimized at $\psi = 136.1°$, 138.2°, 134.8°, 136.1°, 139.1°, and 139.7°, which are optimized values for conformations tFdg$^-$, tFdt, tFug$^-$, tFut, tFug$^+$, and tFdg$^+$ of Ac-Hyp-NMe_2, respectively, at the HF/6-31+G(d) level of theory. [h] Optimized at $\psi = -7.9°$, −10.9°, and −10.2°, which are optimized values for conformations cAdg$^-$, cAdt, and cAdg$^+$ of Ac-Hyp-NHMe, respectively, at the HF/6-31+G(d) level of theory.

TABLE 2: Backbone Torsion Angles, Endocyclic Torsion Angles, and Puckering Amplitudes of Ac-Flp-NHMe Optimized at the HF/6-31+G(d) Level of Theory in the Gas Phase

	backbone torsion angles[a]				endocyclic torsion angles[a]					puckering amplitude	thermodynamic quantities		
conformer[b]	ω'	ϕ	ψ	ω	χ^0	χ^1	χ^2	χ^3	χ^4	q_z[c]	ΔE_e[d]	ΔH[e]	ΔG[f]
tCu	−172.0	−85.7	82.9	−174.6	−10.4	−12.7	30.0	−35.7	29.0	0.343	0.00	0.00	0.11
tCd	−174.1	−85.8	82.0	−174.9	−16.3	31.7	−36.0	25.9	−5.8	0.351	0.11	0.09	0.00
tFu[g]	179.7	−63.9	135.5	−175.5	−1.7	−19.7	33.3	−33.6	22.3	0.340	1.15	0.98	0.55
tFd[g]	177.4	−70.4	136.1	−176.6	−15.9	30.4	−34.4	24.6	−5.3	0.337	1.49	1.40	0.72
cAu	6.8	−79.0	−20.1	−178.1	2.1	−23.1	35.2	−33.6	19.7	0.350	2.78	2.52	2.07
tAu	−168.4	−78.7	−11.1	174.8	1.4	−22.6	34.9	−33.7	20.2	0.348	3.00	2.78	2.39
cAd	8.8	−88.9	−10.1	179.7	−13.0	30.3	−36.9	28.7	−9.7	0.358	3.75	3.56	3.12
tAd[h]	−169.6	−84.1	−10.1	174.0	−8.7	28.5	−37.9	32.3	−14.6	0.369	3.80	3.60	3.10
cFu	−0.6	−59.5	149.8	176.5	4.9	−25.0	35.7	−32.3	17.2	0.350	4.62	4.30	3.47
cFd	−2.2	−75.1	147.9	175.8	−18.0	32.0	−35.0	24.1	−3.6	0.347	5.52	5.27	4.08
ts4	−69.5	−86.1	−6.1	177.7	16.1	−32.8	37.2	−27.7	7.0	0.365	18.17	17.01	17.14
ts1	116.1	−101.6	−13.3	−178.3	9.8	16.3	−35.5	41.4	−31.9	0.399	18.72	17.65	18.08
ts2	116.1	−89.6	−19.9	−174.9	22.8	−36.1	35.7	−22.3	−0.6	0.366	18.95	17.78	18.45
ts3	−66.3	−89.6	−3.4	177.0	8.6	16.6	−34.8	39.4	−30.1	0.384	20.09	18.97	18.64

[a−f] See footnotes *a*−*f* of Table 1. [g] Optimized at $\psi = 135.5°$ and 136.1°, which are optimized values for conformations tFu and tFd of Ac-Flp-NMe_2, respectively, at the HF/6-31+G(d) level of theory. [h] Optimized at $\psi = -10.1°$, which is the optimized value for the conformation cAd at the HF/6-31+G(d) level of theory.

NHMe. In particular, it should be noted that the conformations cAd and cAu are more stabilized by about 2 kcal/mol versus the PPI-like conformations cFd and cFu, which are lower by about 0.5 kcal/mol than that of Ac-Pro-NHMe.[34]

The PESs of Ac-*trans*-Flp-NHMe at the HF/6-31+G(d) level of theory are overall similar to those of Ac-*trans*-Hyp-NHMe. There are one minimum tCd at $\psi = 82°$ for the down-puckered conformation and two minima tAu and tCu at $\psi = -11°$ and 82°, respectively, for the up-puckered conformation (Table 2). The first two lowest-energy conformations tCd and tCu have a common C_7 hydrogen bond between C═O of the N-terminal group and N−H of the C-terminal group, as seen for Ac-Hyp-

NHMe and Ac-Pro-NHMe. The inaccessibility of PPII-like conformations tFd and tFu can be ascribed to this hydrogen bond, as found for Ac-Hyp-NHMe and Ac-Pro-NHMe. However, it should be noted that the up-puckered conformation tCu of Ac-Flp-NHMe becomes more stabilized by 0.1 kcal/mol versus the down-puckered tCd conformation, whereas Ac-Hyp-NHMe prefers the down-puckered conformation tCd by 1.1 kcal/mol versus the up-puckered tCu conformation (Tables 1 and 2). The barriers for conformational transitions of tAu → tCu for Ac-Flp-NHMe at $\psi = 0°$ and $-105°$ are estimated to be 0.03 and 12.8 kcal/mol, which are almost the same as the values of Ac-Hyp-NHMe. The corresponding barriers for down-puckered conformations cannot be estimated because the conformation tAd is not a local minimum, as seen for Ac-Hyp-NHMe.

For the PESs of Ac-*cis*-Flp-NHMe at the HF/6-31+G(d) level of theory, there are two minima cAd and cFd at $\psi = -10°$ and 148°, respectively, for the down-puckered conformation and two minima cAu and cFu at $\psi = -20°$ and 150°, respectively, for the up-puckered conformation (Table 2). In particular, the higher barriers appear at $\psi = 75°$ for the backbone conformation C, which may be ascribed by the unfavorable nonbonded interaction between the methyl carbon of the acetyl group and the C^{α} of the Flp residue and by the weak electrostatic interaction between the carbonyl oxygen of the acetyl group and the carbonyl carbon of the Flp residue, as seen for Ac-Hyp-NHMe. The lack of the C_7 hydrogen bond between the two terminal groups seems to allow the PPI-like conformations cFd and cFu to be feasible. Although the overall shapes of the PESs of Ac-*cis*-Flp-NHMe are similar to those of Ac-*cis*-Hyp-NHMe, the barriers for the transitions cA → cF at $\psi = -120°$ and 75° for down-puckered structures of Ac-Flp-NHMe are lowered by about 1 kcal/mol versus Ac-Hyp-NHMe, and the barrier at $\psi = 75°$ for the up-puckered structures is lowered by 0.5 kcal/mol. In particular, it should be noted that the conformations cAd and cAu are more stabilized by about 2 kcal/mol versus the PPI-like conformations cFd and cFu, as seen for Ac-Hyp-NHMe.

Tables 1 and 2 list the backbone torsion angles, endocyclic torsion angles, and puckering amplitudes of the local minima and transition states for Ac-Hyp-NHMe and Ac-Flp-NHMe optimized at the HF/6-31+G(d) level of theory in the gas phase, respectively. Four representative conformations tCd, tCu, cAu, cAd, and the lowest-energy transition state of Ac-Hyp-NHMe and Ac-Flp-NHMe are presented in Figures 4 and 5, respectively. In Tables 1 and 2, the degree of puckering of the prolyl ring is described in terms of q_z by Cremer and Pople,[60] which is the maximum *z*-displacement perpendicular to the mean plane of the ring. Recently we reported that two other puckering amplitudes, χ_m of Altona and Sundaralingam[61] and q_α of Han and Kang,[62] showed the same trend of puckering along the prolyl cis−trans isomerization of Ac-Pro-NHMe although their absolute values are different.[56] q_α is the maximum angle between the mean plane and the line joining the center of mass and each atom of the ring. χ_m is the maximum value attainable by endocyclic torsion angles of the ring.

The absolute difference (ad) in the backbone torsion angle ϕ of Ac-Hyp-NHMe (Table 1) and Ac-Flp-NHMe (Table 2) from Ac-Pro-NHMe (Table 1 of ref 34) is less than 6° for up-puckered conformations and is negligible for down-puckered conformations at the HF/6-31+G(d) level of theory. As expected from PESs for Ac-Hyp-NHMe (Figure 2), Ac-Flp-NHMe (Figure 3), and Ac-Pro-NHMe (Figure 2 of ref 34), there are no significant differences in the backbone torsion angle ψ of the local minima

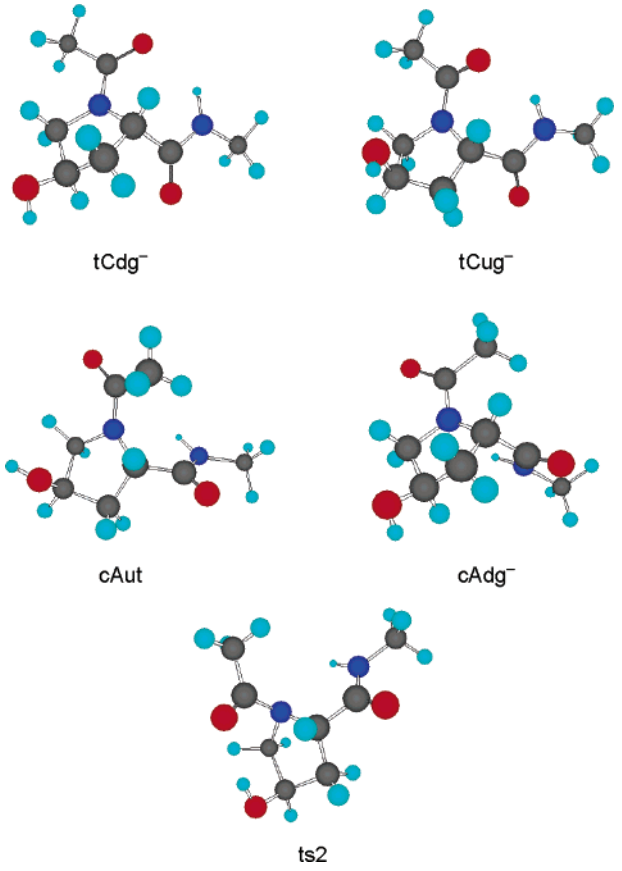

Figure 4. Optimized tCdg⁻, tCug⁻, cAut, cAdg⁻, and ts2 conformations of Ac-Hyp-NHMe at the HF/6-31+G(d) level of theory in the gas phase.

for Pro and 4(*R*)-substituted residues at the HF/6-31+G(d) level of theory, and their ad's remain within 6°, except the decrease of 8° for Ac-Flp-NHMe from Ac-Pro-NHMe. In particular, the ad's for all endocyclic torsion angles $\chi^0-\chi^4$ for local minima of Ac-Hyp-NHMe (Table 1) and Ac-Flp-NHMe (Table 2) from Ac-Pro-NHMe (Table 1 of ref 34) are found to be less than 5°. These calculated ad's for Ac-Hyp-NHMe and Ac-Flp-NHMe from Ac-Pro-NHMe may indicate that the 4(*R*)-substitution did not result in significant changes in backbone torsion angles as well as endocyclic torsion angles of the prolyl ring. The small changes in endocyclic torsion angles imply the small variations in puckering amplitude, as seen in Tables 1 and 2 and Table 1 of ref 34.

By comparison of bond lengths and bond angles of local minima optimized at the HF/6-31+G(d) level of theory for Ac-Hyp-NHMe and Ac-Flp-NHMe with those for Ac-Pro-NHMe, it is known that the bond lengths $r(N-C^{\delta})$, $r(C^{\alpha}-C^{\beta})$, $r(C^{\beta}-C^{\gamma})$, and $r(C^{\gamma}-C^{\delta})$ of the prolyl ring are decreased by 0.001−0.009 Å for most of the local minima for Ac-Hyp-NHMe and Ac-Flp-NHMe. In particular, the bond length $r(C^{\beta}-C^{\gamma})$ for all local minima and the bond length $r(C^{\gamma}-C^{\delta})$ for conformations tCu, cAu, tAu, and cFu are decreased by more than 0.01 Å for Ac-Flp-NHMe. However, there are negligible changes in bond angles for all local minima of Ac-Hyp-NHMe and Ac-Flp-NHMe. However, the small changes in the backbone torsion angles ϕ and ψ and the decrease of the bond lengths $r(C^{\beta}-C^{\gamma})$ or $r(C^{\gamma}-C^{\delta})$ appear to induce the increase of relative stability of the trans up-puckered conformation to the trans down-puckered conformation in the order Ac-Pro-NHMe < Ac-Hyp-NHMe < Ac-Flp-NHMe.

In particular, we could locate four transition states for the trans-to-cis isomerization of Ac-Hyp and Ac-Flp peptide bonds

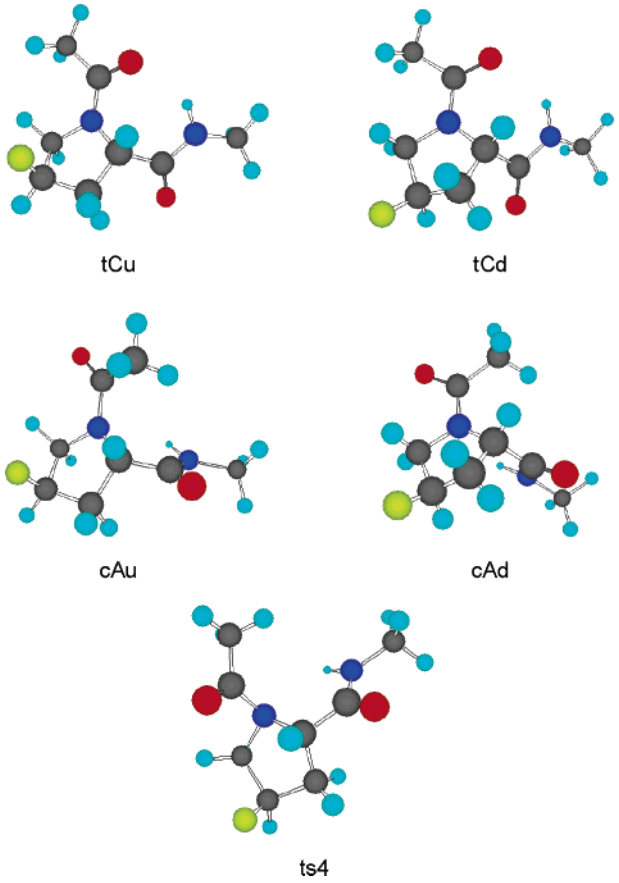

Figure 5. Optimized tCu, tCd, cAu, cAd, and ts4 conformations of Ac-Flp-NHMe at the HF/6-31+G(d) level of theory in the gas phase.

at the HF/6-31+G(d) level of theory, as found for Ac-Pro-NHMe;[34] ts1 and ts2 are similar to syn/exo structures with down and up puckerings, respectively, whereas ts3 and ts4 resemble anti/exo structures with down and up puckerings, respectively, according to the definition of Fischer et al.[63] In comparison to Ac-Pro-NHMe,[34] there are small ad's within 6° in backbone torsion angles ϕ and ψ and within 5° in endocyclic torsion angles for Ac-Hyp-NHMe and Ac-Flp-NHMe, except for the transition state ts2 of Ac-Flp-NHMe. The transition states ts2 and ts4 become the lowest-energy transition states for Ac-Hyp-NHMe and Ac-Flp-NHMe, respectively (Tables 1 and 2). This indicates that the 4(*R*)-substitution did not contribute to change remarkably the structure of the backbone and the prolyl ring but contributed to alter the relative stabilities of the transition states.

From the comparison of bond lengths and bond angles of transition states optimized at the HF/6-31+G(d) level of theory for Ac-Hyp-NHMe with those for Ac-Pro-NHMe, it is found that the bond length $r(N-C^{\alpha})$ becomes shorter by 0.01 Å for the transition state ts1 and longer by 0.02 Å for the transition state ts4 and that the bond length $r(C^{\gamma}-C^{\delta})$ becomes shorter by 0.01 Å for the transition state ts4. For Ac-Flp-NHMe, the bond length $r(N-C^{\delta})$ becomes shorter by 0.03 Å for the transition state ts2, and the bond length $r(C^{\beta}-C^{\gamma})$ becomes shorter by 0.01, 0.02, and 0.01 Å for transition states ts1, ts3, and ts4, respectively, than those of Ac-Pro-NHMe. The bond angles of the transition state structures of Ac-Hyp-NHMe and Ac-Flp-NHMe are almost similar to those of Ac-Pro-NHMe, except some bond angles around the prolyl nitrogen are larger than 3°, which are the bond angle $\theta(C^{\delta}-N-C')$ for transition states ts1 and ts4 of Ac-Hyp-NHMe and for transition states ts2 and ts4 of Ac-Flp-NHMe, the bond angle $\theta(C^{\alpha}-N-C')$ for transition states ts2 and ts4 of Ac-Flp-NHMe, and the bond angle $\theta(N-C^{\delta}-C^{\gamma})$ for the transition state ts2 of Ac-Flp-NHMe.

The backbone torsion angles, endocyclic torsion angles, and puckering amplitudes of the local minima and transition states for Ac-Hyp-NHMe optimized at the B3LYP/6-31+G(d) and B3LYP/6-311++G(d,p) levels of theory in the gas phase are listed in Tables S1 and S2, respectively, of the Supporting Information. The corresponding data for Ac-Flp-NHMe are listed in Tables S3 and S4, respectively, of the Supporting Information. On going from the HF/6-31+G(d) level of theory to the B3LYP/6-31+G(d) and B3LYP/6-311++G(d,p) levels of theory, there are some shifts in the backbone torsion angles ϕ and ψ. For both Ac-Hyp-NHMe and Ac-Flp-NHMe, the local minima tCd, tCu, and tAu have $\Delta\phi > 0$ and $\Delta\psi < 0$, the local minima cAu and cAd have $\Delta\phi < 0$ and $\Delta\psi > 0$, and the local minima cFu and cFd have $\Delta\phi < 0$ and $\Delta\psi < 0$. Transition states ts1, ts2, and ts3 have $\Delta\phi < 0$ and $\Delta\psi > 0$, and the transition state ts4 has $\Delta\phi < 0$ and $\Delta\psi < 0$. Most of the shifts in torsion angles ϕ and ψ are within ±5°, but the local minima tCu, tAu, cAd, cFu, and cFd for both Ac-Hyp-NHMe and Ac-Flp-NHMe have somewhat larger shifts in the torsion angle ψ. However, the changes in endocyclic torsion angles $\chi^0-\chi^4$ are less than 3° for all local minima and transition states for both Ac-Hyp-NHMe and Ac-Flp-NHMe. Small changes in torsion angles for the backbone and the prolyl ring on going from the B3LYP/6-31+G(d) level of theory to the B3LYP/6-311++G-(d,p) level of theory are found, which indicate that the structures optimized at both B3LYP levels are quite similar to each other.

Because no X-ray structures for Ac-Hyp-NHMe and Ac-Flp-NHMe are available, X-ray structures for Ac-Hyp-OMe and Ac-Flp-OMe[17] are compared with our optimized conformations. Methyl esters of prolyl residues have polyproline-like conformations in the crystal,[17] and their preferred conformations were confirmed to be polyproline-like by B3LYP/6-31+G(d) calculations in the gas phase.[19,39] Therefore, the methyl esters of Ac-Pro, Ac-Hyp, and Ac-Flp have been studied as models for the prolyl residues of collagen.[18−20,32] However, it should be noted that the methyl ester group can induce a different pattern of intermolecular hydrogen bonds and packing for the prolyl residues from those with *N*′-methyl or *N*′,*N*′-dimethyl amides in crystal. As a result, the preferred conformations would be different depending on the C-terminal end group. For example, the preferred conformation of Ac-Pro-NHMe in the crystal is the down-puckered tAd (i.e., $\phi = -76°$ and $\psi = -16°$) with the trans prolyl peptide bond,[64] whereas the down-puckered conformation cFd (i.e., $\phi = -79°$ and $\psi = 177°$) with the cis prolyl peptide bond is preferred for Ac-Pro-OMe.[17] In addition, these two proline peptides were known to have different conformations in solution from circular dichroism (CD) and optical rotatory dispersion (ORD) experiments.[65]

According to HF/6-31+G(d) calculations in the gas phase, the most preferred conformations are tCd with $\phi = -86°$ and $\psi = 75°$ for Ac-Pro-NHMe[34] and tFd with $\phi = -71°$ and $\psi = 156°$ for Ac-Pro-OMe.[66] In particular, the most preferred conformation for Ac-Pro-NMe_2, the simplest model for polyproline, is tFd with $\phi = -70°$ and $\psi = 142°$,[35] which are consistent with $\phi = -77°$ and $\psi = 146°$ of an X-ray structure for polyproline II.[67] The X-ray values of (ϕ, ψ) for the conformation tFd of Pro residues in collagen model peptides are (−73°, 163°).[6−8] At the B3LYP/6-31+G(d) level of theory, the optimized values of (ϕ, ψ) for the conformation tFu are (−60°, 141°) and (−59°, 141°) for Ac-Hyp-OMe and Ac-Flp-OMe, respectively,[19,39] whereas they are (−67°, 128°) and (−70°, 126°) for Ac-Hyp-NMe_2 and Ac-Flp-NMe_2, respectively.[68] The

corresponding values from X-ray structures of Ac-Hyp-OMe and Ac-Flp-OMe are (−62°, 156°) and (−55°, 141°), respectively.[17] The X-ray values of (ϕ, ψ) for the conformation tFu of the Hyp residues in collagen model peptides are (−57°, 150°).[6−8] These results indicate that methyl esters of prolyl residues may have polyproline-like structures with somewhat larger ψ by about 10° than *N*′,*N*′-dimethyl amides of prolyl residues but somewhat smaller ψ by about 10° than that of collagen model peptides. Because the preferred conformations of Ac-Hyp-OMe and Ac-Flp-OMe are the same in the crystal but different from that of Ac-Pro-OMe, as discussed above, it is not possible to figure out exactly the structural changes due to the 4(*R*)-substitution. By comparison of structural changes of X-ray structures of Ac-Pro-OMe, Ac-Hyp-OMe, and Ac-Flp-OMe, the electron-withdrawing substituent at the 4(*R*)-position decreased the bond lengths $r(C^{\alpha}-C^{\beta})$, $r(C^{\beta}-C^{\gamma})$, and $r(C^{\gamma}-C^{\delta})$ of the prolyl ring.[17] In particular, the bond length $r(C^{\gamma}-C^{\delta})$ is decreased by 0.013 ± 0.004 Å in Ac-Hyp-OMe and 0.016 ± 0.003 Å in Ac-Flp-OMe.[17] These X-ray results are consistent with our results for local minima optimized at the HF/6-31+G(d) level of theory, as described above.

Relative electronic energies (ΔE_e), enthalpies (ΔH), and Gibbs free energies (ΔG) of local minima and transition states of Ac-Hyp-NHMe optimized at the HF/6-31+G(d), B3LYP/6-31+G(d), and B3LYP/6-311++G(d,p) levels of theory in the gas phase are listed in Tables 1 and Tables S1 and S2 of the Supporting Information, respectively. The corresponding values for Ac-Flp-NHMe are shown in Table 2 and Tables S3 and S4 of the Supporting Information, respectively. The most probable down-puckered conformation tCdg$^-$ of Ac-Hyp-NHMe is more stabilized than the up-puckered conformation tCug$^-$ by 1.05 kcal/mol in ΔE_e and 1.24 kcal/mol in ΔG at the HF/6-31+G(d) level of theory, by 0.49 kcal/mol in ΔE_e and 0.60 kcal/mol in ΔG at the B3LYP/6-31+G(d) level of theory, and by 0.39 kcal/mol in ΔE_e and 0.71 kcal/mol in ΔG at the B3LYP/6-311++G(d,p) level of theory. However, the most probable up-puckered conformation tCu is more preferred than the down-puckered conformation tCd for Ac-Flp-NHMe by 0.11 kcal/mol in ΔE_e and −0.11 kcal/mol in ΔG at the HF/6-31+G(d) level of theory, by 0.91 kcal/mol in ΔE_e and 0.62 kcal/mol in ΔG at the B3LYP/6-31+G(d) level of theory, and by 1.01 kcal/mol in ΔE_e and 0.75 kcal/mol in ΔG at the B3LYP/6-311++G(d,p) level of theory. At the HF/6-31+G(d) level of theory, the down-puckered conformation tCd of Ac-Pro-NHMe is more feasible than the up-puckered conformation tCu by 1.69 kcal/mol in ΔE_e and 1.73 kcal/mol in ΔG.[34] In particular, PPII-like conformations tFd and tFu of Ac-Hyp-NHMe and Ac-Flp-NHMe at $\psi \approx 130°$ have the same preference of prolyl puckerings, although they are not local minima (also see Figures 2 and 3). These relative electronic energies and free energies indicate that the more the prolyl residue prefers the up puckering, the more the electronegativity of the 4(*R*)-substitution increases. This is reasonably consistent with the prolyl puckering of X-ray structures for Ac-Pro-OMe, Ac-Hyp-OMe, and Ac-Flp-OMe,[17] although these methyl esters have different backbone structures from those of the N-methylated amides studied here. In X-ray structures of model peptides for collagen, the Pro residues have down and up puckerings, and the Hyp residue has the up puckering.[6−8]

As mentioned above, the most probable transition states are ts2 and ts4 for prolyl cis−trans isomerization of Ac-Hyp-NHMe and Ac-Flp-NHMe, respectively, whereas the transition state ts1 is most probable for Ac-Pro-NHMe. The transition state ts1 is a down-puckered conformation with $\omega' \approx +120°$, whereas transition states ts2 and ts4 are up-puckered conformations with $\omega' \approx +120°$ and −70°, respectively. This indicates that the cis−trans isomerization proceeds through the clockwise and counterclockwise rotations about the prolyl peptide bond for Ac-Hyp-NHMe and Ac-Flp-NHMe, respectively, at the HF and B3LYP levels of theory. The transition state ts2 of Ac-Hyp-NHMe is more stabilized than the transition state ts1 by 1.94 kcal/mol in ΔE_e and 1.09 kcal/mol in ΔG at the HF/6-31+G(d) level of theory, by 2.89 kcal/mol in ΔE_e and 1.95 kcal/mol in ΔG at the B3LYP/6-31+G(d) level of theory, and by 2.48 kcal/mol in ΔE_e and 1.54 kcal/mol in ΔG at the B3LYP/6-311++G(d,p) level of theory. For Ac-Flp-NHMe, the transition state ts4 is more stabilized than the transition state ts1 by 0.55 kcal/mol in ΔE_e and 0.94 kcal/mol in ΔG at the HF/6-31+G(d) level of theory, by 0.99 kcal/mol in ΔE_e and 1.77 kcal/mol in ΔG at the B3LYP/6-31+G(d) level of theory, and by 0.99 kcal/mol in ΔE_e and 1.47 kcal/mol in ΔG at the B3LYP/6-311++G(d,p) level of theory. As seen for local minima, these results indicate that the more the prolyl residue prefers the up-puckered transition state, the more the electronegativity of the 4(*R*)-substitution increases.

Table 3 lists the populations of the prolyl peptide bond with puckering, rotational barriers, and relative energies of cis conformers for Ac-Pro-NHMe, Ac-Hyp-NHMe, and Ac-Flp-NHMe calculated at the HF/6-31+G(d), B3LYP/6-31+G(d),

TABLE 3: Populations of Prolyl Peptide Bond with Puckering, Rotational Barriers, and Relative Energies of Cis Conformers for Ac-Pro-NHMe, Ac-Hyp-NHMe, and Ac-Flp-NHMe Calculated at the HF/6-31+G(d), B3LYP/6-31+G(d), and B3LYP/6-311++G(d,p) Levels of Theory in the Gas Phase[a]

	prolyl peptide bond/puckering[b]				rotational barrier[c,d]		relative energy[c,e]
dipeptide	trans/down	trans/up	cis/down	cis/up	$\Delta G_{tc}^{\ddagger}$	$\Delta G_{ct}^{\ddagger}$	$\Delta G_{c/t}$
			HF/6-31+G(d)				
Pro[f]	92.5	5.6	1.7	0.3	17.62	15.25	2.37
	89.2	5.2	4.4	1.2	16.97	15.16	1.81
Hyp	81.0	18.4	0.2	0.4	16.95	13.65	3.30
	82.6	15.1	0.9	1.5	17.07	14.44	2.63
Flp	45.2	54.3	0.1	0.4	18.17	15.39	2.78
	53.0	44.9	0.3	1.8	17.14	15.07	2.07
			B3LYP/6-31+G(d)				
Hyp	59.5	40.3	0.1	0.1	18.31	14.28	4.03
	62.7	36.1	0.6	0.6	18.37	15.22	3.16
Flp	17.7	82.2	0.0	0.1	20.70	16.53	4.17
	25.6	73.1	0.2	1.1	19.15	16.64	2.51
			B3LYP/6-311++G(d,p)				
Hyp	56.6	43.2	0.1	0.1	18.24	14.43	3.81
	65.9	33.1	0.2	0.7	18.46	15.40	3.06
Flp	15.4	84.5	0.0	0.1	20.35	16.30	4.05
	21.9	77.5	0.1	0.5	19.20	16.18	3.02

[a] The values in the first and second rows for each dipeptide were computed using the relative electronic energy (ΔE_e) and Gibbs free energy (ΔG) of each local minimum in Tables 1 and 2 and Tables S1−S4 of the Supporting Information, respectively. [b] Populations (%) were calculated using the Boltzmann statistical weights at 25 °C, depending on the trans/cis prolyl peptide bond and down/up puckerings. According to potential energy surfaces of Ac-Hyp-NHMe and Ac-Flp-NHMe in the gas phase, shown in Figures 2 and 3, the nonlocal minima such as the conformers tAd, tFd, and tFu were excluded in computing the populations. [c] Units in kcal/mol; the lowest electronic energy or Gibbs free energy for each of the trans, cis, and transition state conformations was used for these calculations. Free energies were calculated at 25 °C. [d] $\Delta G_{tc}^{\ddagger}$ and $\Delta G_{ct}^{\ddagger}$ represent the barriers for the trans-to-cis and cis-to-trans rotations for the Ac−Xaa (Xaa = Pro, Hyp, and Flp) peptide bond, respectively. [e] $\Delta G_{c/t}$ is the electronic energy or Gibbs free energy of the cis conformer relative to the trans conformer. [f] Calculated from relative electronic energies and Gibbs free energies of Ac-Pro-NHMe in ref 34.

and B3LYP/6-311++G(d,p) levels of theory in the gas phase. At the HF/6-31+G(d) level of theory, the populations of the down-puckered conformations with the trans prolyl peptide bond calculated using relative electronic energies and free energies decrease in the order Ac-Pro-NHMe > Ac-Hyp-NHMe > Ac-Flp-NHMe, and the populations of the up-puckered conformations with the trans prolyl peptide bond increase in the reverse order. At the B3LYP/6-31+G(d) and B3LYP/6-311++G(d,p) levels of theory, the preference to up puckering of Hyp and Flp residues increases more, which may be ascribed to the larger relative stabilities of the up-puckered conformations at the B3LYP levels than the HF level, as described above.

The increase in the population of the trans up-puckered conformers for Ac-Flp-OMe versus Ac-Pro-OMe was interpreted as the $n \rightarrow \pi^*$ interaction between the carbonyl oxygen preceding the prolyl residue and the carbonyl carbon of the prolyl residue by natural bond orbital (NBO) analysis at the B3LYP/6-31+G(d) level of theory.[19] The distance d(C═O···C) between the carbonyl oxygen preceding the prolyl residue and the carbonyl carbon of the prolyl residue was used as a measure of the strength for the $n \rightarrow \pi^*$ interaction for Ac-Pro-OMe and Ac-Flp-OMe. The change of the distance d(C═O···C) from the conformation tFd to the conformation tFu was calculated to be −0.37 and −0.19 Å for Ac-Flp-OMe and Ac-Pro-OMe at the B3LYP/6-31+G(d) level of theory, respectively.[19] The relatively larger distance change in Ac-Flp-OMe than that in Ac-Pro-OMe was attributed to the increase in the relative stability of the trans up-puckered polyproline-like conformation.[19,20] However, the intramolecular hydrogen-bonded conformations tCd and tCu mostly preferred trans conformations for all three Ac-Pro-NHMe, Ac-Hyp-NHMe, and Ac-Flp-NHMe, as described above. The distances d(C═O···C) are computed to be longer than 3.25 Å for both the conformations tCd and tCu of these three N-methylated amides at all HF and B3LYP levels of theory. In particular, the change of the distance from conformation tCd to conformation tCu was calculated to be about −0.05 Å for Ac-Pro-NHMe and about −0.03 Å for Ac-Hyp-NHMe and Ac-Flp-NHMe. Therefore, these results may indicate that the only $n \rightarrow \pi^*$ interaction between two adjacent carbonyl groups cannot explain the increased stability of the trans up-puckered conformations for N-methylated amides as the electronegativity of 4(*R*)-substitution increases.

At the HF/6-31+G(d) level of theory, the rotational barriers to prolyl trans-to-cis and cis-to-trans isomerizations for Ac-Hyp-NHMe are lowered by 0.7 and 1.6 kcal/mol in ΔE_e and 0.1 and 0.7 kcal/mol in ΔG, respectively, versus those of Ac-Pro-NHMe. However, the rotational barriers to trans-to-cis isomerization for Ac-Flp-NHMe are increased by 0.6 kcal/mol in ΔE_e and 0.2 kcal/mol in ΔG versus those of Ac-Pro-NHMe. On going from the HF/6-31+G(d) level of theory to the B3LYP/6-31+G(d) and B3LYP/6-311++G(d,p) levels of theory, the rotational barriers to trans-to-cis and cis-to-trans isomerizations for Ac-Hyp-NHMe are increased by about 1 kcal/mol in ΔE_e and ΔG versus those for Ac-Pro-NHMe. For Ac-Flp-NHMe, the rotational barriers to trans-to-cis isomerization are increased by about 2 kcal/mol in ΔE_e and ΔG versus those for Ac-Pro-NHMe.

The relative electronic energy and free energy of the most probable cis conformation to the most probable trans conformation increase for each of Ac-Hyp-NHMe and Ac-Flp-NHMe versus those of Ac-Pro-NHMe at the HF/6-31+G(d) level of theory. These relative electronic energies and free energies increase more at the B3LYP/6-31+G(d) and B3LYP/6-311++G(d,p) levels of theory.

Intramolecular Hydrogen Bond in Transition States. A comparative study on rotational barriers has been undertaken for two sterically similar prolines in organic and in aqueous/organic solution; one proline contains the catalytic N−H amide group, and the other has the ester end group.[69] The kinetic and spectroscopic results have been interpreted as the evidence that indicates the existence of an intramolecular hydrogen bond between the prolyl nitrogen and the following amide N−H group, which is capable of catalyzing the prolyl cis−trans isomerization by up to 260-fold in model peptides.[69] The existence of this hydrogen bond and its role in prolyl isomerization has been also proposed on the basis of the adiabatic energy map of a proline dipeptide at the HF/6-31G(d)//HF/3-21G level of theory.[63] In particular, we suggested the role of this hydrogen bond in prolyl isomerization of *N*′-methyl amides of proline,[55] pseudo-proline,[57] and 5-methylated prolines.[58] The distances $d(N_{Pro}\cdots H-N_{NHMe})$ between the prolyl nitrogen and the following hydrogen of the NHMe group calculated at the HF/6-31+G(d) level of theory are 2.27, 2.27, and 2.30 Å for transition states ts1 of Ac-Pro-NHMe, ts2 of Ac-Hyp-NHMe, and ts4 of Ac-Flp-NHMe, respectively. The corresponding values for Ac-Hyp-NHMe and Ac-Flp-NHMe are 2.18 and 2.25 Å at the B3LYP/6-31+G(d) level of theory and 2.17 and 2.22 Å at the B3LYP/6-311++G(d,p) level of theory, respectively.

In particular, the sum (S) of three bond angles (i.e., C′−N−C^{γ}, C′−N−C^{α}, and C^{γ}−N−C^{α}) around the nitrogen of the prolyl ring can be used to identify the degree of planarity at the imide nitrogen. If the quantity δ is defined as $S - 360°$, then the imide nitrogen is nearly planar in the sp^2 bonding state when $\delta \approx 0°$. As the quantity δ becomes more negative, the degree of nonplanarity (i.e., the pyramidal sp^3 character) of the imide nitrogen increases more. The experimental bond angles of H−N−H for ammonia and C−N−C for trimethylamine are 107.8° and 110.9°, respectively.[70] The values of δ for ammonia and trimethylamine can be estimated to be −36.6° and −27.3°, respectively. This indicates that the nitrogens of ammonia and trimethylamine are pyramidal. However, the sum of the three C−N−C bond angles of *N*,*N*-dimethylformamide determined from gas-phase electron diffraction[71] is 354.6°, and the value of δ is −5.4°; i.e., the imide nitrogen is nearly planar. The values of δ for the transition state ts1 of Ac-Pro-NHMe,[34] ts2 of Ac-Hyp-NHMe, and ts4 of Ac-Flp-NHMe are calculated to be −23.5°, −23.7°, and −15.9° at the HF/6-31+G(d) level of theory, respectively. The computed values of δ for the transition state ts2 of Ac-Hyp-NHMe and ts4 of Ac-Flp-NHMe are −26.0° and −19.4° at the B3LYP/6-31+G(d) level of theory and −26.1° and −19.2° at the B3LYP/6-311++G(d,p) level of theory, respectively. The calculated values of δ for the transition state ts1 of Ac-Pro-NHMe[34] and ts2 of Ac-Hyp-NHMe are almost the same as the experimental value of trimethylamine.[70] These results indicate that the imide nitrogens of the Pro and Hyp residues have more pyramidal character than the Flp residue. Thus, the pertinent distance $d(N_{Pro}\cdots H-N_{NHMe})$ and the pyramidality of the imide nitrogen for the transition states could be used in describing the changes in the barrier to prolyl cis−trans isomerization. Although these two quantities can explain why Ac-Flp-NHMe has higher rotational barriers than Ac-Pro-NHMe and Ac-Hyp-NHMe, they fail to explain the lower rotational barriers of Ac-Hyp-NHMe versus Ac-Pro-NHMe.

Conformations in Solution. The PESs of Ac-Hyp-NHMe and Ac-Flp-NHMe along the angle ψ at the HF/6-31+G(d) level with the CPCM-UAHF(G98) method in chloroform and water are shown in Figures 2 and 3, respectively. For Ac-*trans*-Hyp-NHMe and Ac-*trans*-Flp-NHMe in chloroform, the relative

TABLE 4: Comparison of Cis Populations (%) for Ac-Pro-NHMe, Ac-Hyp-NHMe, and Ac-Flp-NHMe Computed with the CPCM-UAHF(G98) and CPCM-UAKS(G03) Methods at the HF/6-31+G(d) Level of Theory in Solution[a]

	CPCM-UAHF(G98)						CPCM-UAKS(G03)					
	HF/6-31+G(d)		B3LYP/6-31+G(d)		B3LYP/6-311++G(d,p)		HF/6-31+G(d)		B3LYP/6-31+G(d)		B3LYP/6-311++G(d,p)	
dipeptide	$CHCl_3$	water	$CHCl_3$	water	$CHCl_3$	water	$CHCl_3$	water	$CHCl_3$	water	$CHCl_3$	water
Pro[b]	11.0	32.9					6.6	25.6				
	21.2	49.2					17.0	51.5				
Hyp	8.9	29.6	4.1	45.3	3.6	35.6	8.7	31.6	3.3	49.0	3.1	34.1
	17.5	45.7	27.6	64.6	22.2	60.6	19.8	55.8	22.6	76.3	20.8	80.1
Flp	6.9	17.0	3.3	35.6	4.0	30.9	7.2	37.6	3.2	75.2	3.3	69.7
	14.5	30.1	25.7	66.4	16.2	43.4	16.2	58.2	24.9	93.4	13.8	86.6

[a] For the definition of CPCM-UAHF(G98) and CPCM-UAKS(G03), see footnote *a* of Table S5 of the Supporting Information. The values in the first and second rows for each dipeptide were calculated using relative total free energies ΔG_{tot}^0 and ΔG_{tot}, respectively; (a) the relative total free energy ΔG_{tot}^0 was computed by the sum of the relative electronic energy (ΔE_e) and the relative solvation free energy ($\Delta\Delta G_s$), and (b) the relative total free energy ΔG_{tot} was computed by the sum of the relative Gibbs free energy (ΔG) and $\Delta\Delta G_s$. The values of ΔE_e and ΔG were taken from Tables 1 and 2 and Tables S1−S4 of the Supporting Information, and those of $\Delta\Delta G_s$ were computed from data of Tables S5 and S6 of the Supporting Information. Populations were calculated using the Boltzmann statistical weights at 25 °C. [b] At the HF/6-31+G(d) level of theory, the values of Ac-Pro-NHMe computed with CPCM-UAHF(G98) were taken from ref 34, and those with CPCM-UAKS(G03) were calculated in this work.

stabilities of the conformations tCd and tCu decreased, the potential well of the conformation tAu became deeper, and three new local minima for conformations tAd, tFd, and tFu appeared, as seen for Ac-Pro-NHMe.[34] In particular, the up-puckered conformations tAu and tFu for Ac-Flp-NHMe were more stabilized in chloroform. In water, the potential wells for the α-helical conformations tAd and tAu as well as the polyproline-like conformations tFd and tFu became deeper, and the conformation tCu disappeared for both Ac-Hyp-NHMe and Ac-Flp-NHMe. In particular, the relative stability of the conformation tCd was remarkably diminished, which may be ascribed to the fact that the hydration of C═O of the N-terminal group and N−H of the C-terminal group became more favorable and the hydrogen bond between them became weaker. This is consistent with CD and NMR experiments on the proline dipeptide.[72] The PESs of Ac-*cis*-Hyp-NHMe and Ac-*cis*-Flp-NHMe in chloroform and water are quite similar to those in the gas phase in Figures 2 and 3, except for that the polyproline-like conformations cFd and cFu became more feasible from the gas phase to chloroform to water, as seen for Ac-Pro-NHMe.[34]

The solvation free energies (ΔG_s) of local minima and transition states optimized at the HF/6-31+G(d), B3LYP/6-31+G(d), and B3LYP/6-311++G(d,p) levels of theory for Ac-Hyp-NHMe and Ac-Flp-NHMe calculated using the CPCM-UAHF(G98) and CPCM-UAKS(G03) methods at the HF/6-31+G(d) level of theory in chloroform and water are summarized in Tables S5 and S6, respectively, of the Supporting Information. The magnitudes of the solvation free energies of local minima and transition states for both Ac-Hyp-NHMe and Ac-Flp-NHMe calculated using the CPCM-UAKS(G03) method increase more than those calculated using the CPCM-UAHF(G98) method, except for some transition states.

Basically, most of the solvation models have been developed and revised to reproduce well experimental transfer free energies of solutes from the gas phase to aqueous solution. The CPCM method has also been modeled to reproduce hydration free energies of various organic solutes.[51] Recently, relative total free energies ΔG_{tot}^0, given by the sum of the relative electronic energies and the relative solvation free energies calculated using the CPCM-UAHF(G98) method at the HF/6-31+G(d) level of theory, predicted well the experimental populations of backbone and cis conformations for Ac-Pro-NHMe[34] and Ac-Pro-NMe_2[35] as well as the experimental rotational barriers about the C−N bond of amides[53] in chloroform and water. In addition, the CPCM-UAKS(G03) calculations for a number of neutral and charged organic molecules at the HF/6-31+G(d)//HF/6-31+G(d) and HF/6-31+G(d)//B3LYP/6-31+G(d) levels of theory provided hydration free energies in agreement with available experimental data.[54] This is the main reason two CPCM methods are employed to calculate solvation free energies in this work.

To select the reasonable solvation model and expression for total free energy in describing the conformational preference and prolyl cis−trans isomerization, the prolyl cis populations of local minima for Ac-Pro-NHMe, Ac-Hyp-NHMe, and Ac-Flp-NHMe optimized at the HF/6-31+G(d), B3LYP/6-31+G(d), and B3LYP/6-311++G(d,p) levels of theory were computed using two CPCM-UAHF(G98) and CPCM-UAKS(G03) methods at the HF/6-31+G(d) level of theory in chloroform and water, which are shown in Table 4. Experimental cis populations for Ac-Pro-NHMe were reported as 14%[65] and 15 ± 4%[73] in chloroform, and 24 ± 4%[73] and 27 ± 3%[74] in water. The experimental cis population of Ac-Hyp-NHMe in water was reported as 21 ± 3%.[75] Although experimental values are too limited to compare with computed cis populations, the relative free energy ΔG_{tot}^0, given by the sum of the relative electronic energy and the relative solvation free energy calculated using the CPCM-UAHF(G98) method for local minima optimized at the HF/6-31+G(d) level of theory, appears to be the best model to reproduce experimental data. In addition, the relative free energy ΔG_{tot}^0 and the relative free energy ΔG_{tot}, given by the sum of the relative electronic energy and the relative solvation free energy computed using the CPCM-UAKS(G03) method for local minima optimized at the HF/6-31+G(d) level of theory, provided good cis populations of Ac-Pro-NHMe in water and chloroform, respectively. In particular, the experimental data indicate the decrease of the cis population on going from Ac-Pro-NHMe to Ac-Hyp-NHMe in water, with which only the relative free energy ΔG_{tot}^0 with the CPCM-UAHF(G98) method is consistent. Therefore, the relative free energy ΔG_{tot}^0 with the CPCM-UAHF(G98) method for local minima optimized at the HF/6-31+G(d) level of theory can be reasonably used in describing the conformational preference and prolyl cis−trans isomerization in solutions.

Populations of Backbone Conformations and Cis−Trans Isomerization in Solution. Calculated populations of the prolyl peptide bond depending on puckering for Ac-Pro-NHMe, Ac-Hyp-NHMe, and Ac-Flp-NHMe from relative free energies ΔG_{tot}^0 with the CPCM-UAHF(G98) method for local minima optimized at the HF/6-31+G(d) level of theory are presented in Table 5. The populations of trans up-puckered conformations increase in the order Ac-Pro-NHMe < Ac-Hyp-NHMe < Ac-Flp-NHMe in chloroform and water, whereas those of trans

TABLE 5: Populations of the Prolyl Peptide Bond with Puckering for Ac-Pro-NHMe, Ac-Hyp-NHMe, and Ac-Flp-NHMe Calculated at the HF/6-31+G(d) Level of Theory in the Gas Phase and in Solution[a]

		Ac-Pro-NHMe[b]			Ac-Hyp-NHMe[c,d]			Ac-Flp-NHMe[c,e]		
conformer		gas	chloroform	water	gas	chloroform	water	gas	chloroform	water
trans/down	tCd	92.5	39.7	0.8	81.0	26.4	0.4	45.2	17.2	0.0
	tFd	0.0	18.7	17.8	0.0	21.0	9.0	0.0	14.9	5.5
	tAd	0.0	12.8	23.9	0.0	5.3	15.6	0.0	1.5	10.3
	sum	92.5	71.3	42.5	81.0	52.8	24.9	45.2	33.6	15.8
trans/up	tCu	5.4	0.0	0.0	18.1	0.0	0.0	54.0	0.0	0.0
	tFu	0.0	12.9	21.5	0.0	29.5	32.0	0.0	50.4	51.1
	tAu	0.2	4.8	3.1	0.3	9.0	13.5	0.3	7.8	16.1
	sum	5.6	17.7	24.6	18.4	38.5	45.5	54.3	58.2	67.2
cis/down	cFd	0.0	1.4	6.6	0.0	1.0	6.1	0.0	0.6	3.7
	cAd	1.7	7.5	19.3	0.2	3.0	15.6	0.1	0.7	2.3
	sum	1.7	9.0	25.9	0.2	4.1	21.7	0.1	1.3	6.0
cis/up	cFd	0.0	0.7	5.7	0.0	1.8	4.2	0.0	3.1	4.8
	cAd	0.3	1.3	1.3	0.4	3.0	3.7	0.4	3.7	6.2
	sum	0.3	2.1	7.0	0.4	4.8	7.8	0.4	6.9	11.0

[a] Units in percent; populations were calculated using the Boltzmann statistical weights at 25 °C. For computation of each statistical weight in the gas phase and in solution, the relative electronic energy (ΔE_e) and the relative total free energy (ΔG_{tot}^0) were used, respectively. See footnote *a* of Table 4 for the definition of ΔG_{tot}^0. Each sum of the populations in the gas phase is also shown in Table 3. [b] Calculated using data of Table 2 in ref 34. [c] According to potential energy (or free energy) surfaces in the gas phase and solution, shown in Figures 2 and 3, the nonlocal minima such as the conformers tAd, tFd, and tFu in the gas phase and the conformer tCu in water were excluded in computing the populations. [d] The values of ΔE_e in Table 1 and ΔG_s calculated with the CPCM-UAHF(G98) method at the HF/6-31+G(d) level of theory in Table S5 of the Supporting Information were used to compute the populations. [e] The values of ΔE_e in Table 2 and ΔG_s calculated with the CPCM-UAHF(G98) method at the HF/6-31+G(d) level of theory in Table S6 of the Supporting Information were used to compute the populations.

TABLE 6: Populations of Backbone Conformations, Rotational Barriers, and Relative Energies of Cis Conformers for Ac-Pro-NHMe, Ac-Hyp-NHMe, and Ac-Flp-NHMe Calculated at the HF/6-31+G(d) Level of Theory in the Gas Phase and in Solution

	backbone[a]							rotational barrier[b,c]		relative energy[b,d]
solvent	tF[e]	cF[e]	F[e]	A	C	cis[f]	experimental cis[f]	$\Delta G_{tc}^{\ddagger}$	$\Delta G_{ct}^{\ddagger}$	$\Delta G_{c/t}$
							Ac-Pro-NHMe[g]			
gas phase	0.0	0.0	0.0	2.1	97.8	2.0		17.62	15.25	2.37
chloroform	31.7	2.2	33.8	26.4	39.7	11.0	14,[h] 15 ± 4[i]	17.51	16.52	0.99
water	39.2	12.3	51.6	47.6	0.8	32.9	24 ± 4,[i] 27 ± 3,[j] 18 ± 5[k]	18.96 (20.4,[j] 21.1,[l] 21.1[m])	18.84 (19.8,[j] 20.7,[l] 20.2[m])	0.13 (0.6,[j] 0.4,[l] 0.9[m])
							Ac-Hyp-NHMe			
gas phase	0.0	0.0	0.0	0.9	99.1	0.7		16.95	13.65	3.30
chloroform	50.5	2.8	53.3	20.3	26.4	8.8		16.87	15.34	1.53
water	41.0	10.3	51.3	48.3	0.4	29.6	21 ± 3,[n] 14 ± 5[k]	19.47 (21.1[l])	18.83 (21.0[l])	0.64 (1.0[l])
							Ac-Flp-NHMe			
gas phase	0.0	0.0	0.0	0.9	99.1	0.6		18.17	15.39	2.78
chloroform	65.3	3.8	69.0	13.8	17.2	8.2		18.31	16.77	1.54
water	56.6	8.5	65.1	34.9	0.0	17.0	13 ± 5[k]	19.24 (20.9[m])	17.99 (19.7[m])	1.25 (1.2[m])

[a] Units in percent; computed using the populations of Table 5. [b] Units in kcal/mol; the values in the gas phase were taken from those computed at the HF/6-31+G(d) level of theory in Table 3. The relative free energies in chloroform and water correspond to the relative total free energies ΔG_{tot}^0, defined in footnote *a* of Table 4, computed at the HF/6-31+G(d) level of theory. Experimental values are listed in parentheses. [c] See footnote *d* of Table 3. [d] See footnote *e* of Table 3. [e] tF and cF conformers correspond to polyproline II and I structures, respectively. The population of F conformer is a sum of those of the tF and cF conformers. [f] Cis Ac−Xaa peptide bond. [g] The calculated values for Ac-Pro-NHMe in the gas phase, chloroform, and water are taken from ref 34. [h] From ref 65. [i] From ref 73. [j] From ref 74. [k] For Ac-Xaa-OMe, Xaa = Pro, Hyp, and Flp; from ref 18. [l] For Ac-Xaa-OMe, Xaa = Pro and Hyp; from ref 32. [m] For Ac-Xaa-OMe, Xaa = Pro and Flp; from ref 33. [n] From ref 75.

down-puckered conformations decrease in the reverse order, as seen in the gas phase. The increase in the populations for trans up-puckered conformations is attributed to the increase in the populations for the PPII-like conformation tFu in solution, as seen for the PESs of Figures 2 and 3. These calculated results on the preference of the trans up-puckered conformation are consistent with the experimental finding that the trans up-puckered conformations of the Hyp and Flp residues are preferred in the crystal[17] and solution.[18,32] In the same manner, the populations of the cis down-puckered conformations decrease, and the populations of the cis up-puckered conformations somewhat increase in solution. In particular, the preference of the trans up-puckered conformations in solution increases more as the increase of solvent polarity, i.e., on going from chloroform to water.

In Table 6, populations of backbone conformations, rotational barriers, and relative energies of cis conformers for Ac-Pro-NHMe, Ac-Hyp-NHMe, and Ac-Flp-NHMe calculated at the HF/6-31+G(d) level of theory in the gas phase and in solution are summarized. In the gas phase, the conformation tCu becomes more populated in the order Ac-Pro-NHMe < Ac-Hyp-NHMe < Ac-Flp-NHMe with the increase of electron-withdrawing ability, but the net population of the conformation C remains dominant for all three residues. The conformations tCd and tCu are stabilized by an intramolecular hydrogen bond between C═O of the N-terminal group and N−H of the C-terminal group, as mentioned above. In chloroform, the population of the polyproline-like conformation F increases with the increase of electron-withdrawing ability, to which the conformation tFu contributes, whereas the population of the α-helical conformation A decreases, which is ascribed to the decrease in populations for conformations tAd and cAd. In water, the polyproline-like conformation F for all three residues is most feasible, although its population is somewhat diminished for Ac-Pro-NHMe and

Ac-Hyp-NHMe due to the increase in population of the α-helical conformation A. In water, the population of polyproline-like conformation F for Ac-Hyp-NHMe is similar to that of Ac-Pro-NHMe, but the population of polyproline-like conformation F for Ac-Flp-NHMe is larger than those of Ac-Pro-NHMe and Ac-Hyp-NHMe.

The calculated cis populations for Ac-Pro-NHMe, Ac-Hyp-NHMe, and Ac-Flp-NHMe increase with the increase of solvent polarity. The cis populations decrease in the order Ac-Pro-NHMe < Ac-Hyp-NHMe < Ac-Flp-NHMe with the increase of electron-withdrawing ability in chloroform and water. In particular, the cis populations for Ac-Pro-NHMe, Ac-Hyp-NHMe, and Ac-Flp-NHMe in water are computed to be 32.9%, 29.6%, and 17.0%, respectively, which are well correlated with experimental data of 18 ± 5%, 14 ± 5%, 13 ± 5% for Ac-Pro-OMe, Ac-Hyp-OMe, and Ac-Flp-OMe, respectively.[18]

The barriers $\Delta G_{ct}^{\ddagger}$ to prolyl cis-to-trans isomerization for Ac-Hyp-NHMe and Ac-Flp-NHMe increase with the increase of solvent polarity, as seen for Ac-Pro-NHMe.[34,42,55] The barriers $\Delta G_{tc}^{\ddagger}$ to trans-to-cis isomerization for Ac-Hyp-NHMe become somewhat lower in chloroform but higher in water. However, the barriers $\Delta G_{tc}^{\ddagger}$ for Ac-Flp-NHMe become higher with the increase of solvent polarity. The barriers $\Delta G_{ct}^{\ddagger}$ and $\Delta G_{tc}^{\ddagger}$ are in the order Ac-Hyp-NHMe < Ac-Pro-NHMe < Ac-Flp-NHMe in chloroform. However, the barriers $\Delta G_{tc}^{\ddagger}$ are in the order Ac-Pro-NHMe < Ac-Flp-NHMe < Ac-Hyp-NHMe, and the barriers $\Delta G_{ct}^{\ddagger}$ are in the order Ac-Flp-NHMe < Ac-Hyp-NHMe ≈ Ac-Pro-NHMe in water. The difference in the order of barriers $\Delta G_{ct}^{\ddagger}$ and $\Delta G_{tc}^{\ddagger}$ in solution may be ascribed to the different transition state structures for Ac-Pro-NHMe, Ac-Hyp-NHMe, and Ac-Flp-NHMe. In the gas phase, the cis−trans isomerization proceeds through clockwise, clockwise, and counterclockwise rotations about the prolyl peptide bond for Ac-Pro-NHMe, Ac-Hyp-NHMe, and Ac-Flp-NHMe, respectively, as discussed above. However, the most probable transition states for Ac-Pro-NHMe, Ac-Hyp-NHMe, and Ac-Flp-NHMe are ts1, ts2, and ts2 in chloroform and ts2, ts1, and ts1 in water, respectively. This indicates that the cis−trans isomerization of three prolyl residues proceeds through the clockwise rotation in solution. The calculated orders of barriers $\Delta G_{ct}^{\ddagger}$ and $\Delta G_{tc}^{\ddagger}$ in water are reasonably consistent with experimental results for Ac-Pro-OMe, Ac-Hyp-OMe, and Ac-Flp-OMe.[32,33] By analysis of the contributions to rotational barriers for prolyl cis−trans isomerization, the isomerization of Ac-Hyp-NHMe and Ac-Flp-NHMe has proven to be entirely enthalpy-driven in the gas phase, chloroform, and water, to which the electronic energies have considerably contributed, as seen for *N*′-methyl amides of proline,[34,42,55] pseudo-proline,[57] and 5-methylated prolines.[58] This is consistent with the experimental results on methyl esters of the Pro, Hyp, and Flp residues[32,33] as well as proline-containing peptides,[76] determined kinetically as a function of temperature. In addition, the relative free energies $\Delta G_{c/t}$ of the most probable cis conformation to the most probable trans conformation were reduced with the increase in solvent polarity, as seen for the cis populations above. The relative stability of the cis conformation is in the order Ac-Hyp-NHMe ≈ Ac-Flp-NHMe > Ac-Pro-NHMe in chloroform and in the order Ac-Pro-NHMe > Ac-Hyp-NHMe > Ac-Flp-NHMe in water. The calculated relative free energies $\Delta G_{c/t}$ for Ac-Pro-NHMe, Ac-Hyp-NHMe, and Ac-Flp-NHMe are consistent with experimental values for methyl esters of the Pro, Hyp, and Flp residues.[32,33] In particular, the increase in the population for PPII-like conformations with up puckering in the order Pro < Hyp < Flp in water may contribute to stabilize the triple helices of $(\text{ProXaaGly})_n$ sequences in the order $(\text{ProProGly})_n$ < $(\text{ProHypGly})_n$ < $(\text{ProFlpGly})_n$, which has been known from thermal stability experiments.[12,13]

Conclusions

The 4(*R*)-substitution by electron-withdrawing groups did not result in significant changes in backbone torsion angles as well as endocyclic torsion angles of the prolyl ring. However, the small changes in backbone torsion angles ϕ and ψ and the decrease of the bond lengths $r(C^{\beta}-C^{\gamma})$ or $r(C^{\gamma}-C^{\delta})$ appear to induce the increase in relative stability of the trans up-puckered conformation and to alter the relative stabilities of transition states for prolyl cis−trans isomerization. On going from the HF/6-31+G(d) level of theory to the B3LYP/6-31+G(d) to the B3LYP/6-311++G(d,p) levels of theory, there are some shifts in backbone torsion angles ϕ and ψ for local minima and transition states for both Ac-Hyp-NHMe and Ac-Flp-NHMe.

The population of trans up-puckered conformations increases in the order Ac-Pro-NHMe < Ac-Hyp-NHMe < Ac-Flp-NHMe in chloroform and water. The increase in population for trans up-puckered conformations in solution is attributed to the increase in population for the PPII-like conformations with up puckering. The barriers $\Delta G_{ct}^{\ddagger}$ to prolyl cis-to-trans isomerization for Ac-Hyp-NHMe and Ac-Flp-NHMe increase with the increase in solvent polarity, as seen for Ac-Pro-NHMe. In particular, it was identified that the cis−trans isomerization proceeds through the clockwise rotation about the prolyl peptide bond for Ac-Hyp-NHMe and Ac-Flp-NHMe in chloroform and water, as seen for Ac-Pro-NHMe. By analysis of the contributions to rotational barriers to prolyl cis−trans isomerization, the isomerization of Ac-Hyp-NHMe and Ac-Flp-NHMe has proven to be entirely enthalpy-driven in the gas phase, chloroform, and water, as seen for Ac-Pro-NHMe. The increase in population for the PPII-like conformations with up puckering in the order Pro < Hyp < Flp in water may contribute to stabilize the triple helices of $(\text{ProXaaGly})_n$ sequences in the order $(\text{ProProGly})_n$ < $(\text{ProHypGly})_n$ < $(\text{ProFlpGly})_n$, which has been known from thermal stability experiments.

Acknowledgment. This work was supported by a grant from Chungbuk National University in 2005.

Supporting Information Available: Backbone torsion angles, endocyclic torsion angles, and puckering amplitudes of Ac-Hyp-NHMe and Ac-Flp-NHMe optimized at the B3LYP/6-31+G(d) and B3LYP/6-311++G(d,p) levels of theory in the gas phase, and solvation free energies (ΔG_s) of Ac-Hyp-NHMe and Ac-Flp-NHMe computed with the CPCM-UAHF(G98) and CPCM-UAKS(G03) methods at the HF/6-31+G(d) level of theory in solution. This material is available free of charge via the Internet at http://pubs.acs.org.

References and Notes

(1) Ramachandran, G. N.; Kartha, G. *Nature* **1955**, *176*, 593.
(2) Rich, A.; Crick, F. H. C. *Nature* **1955**, *176*, 915.
(3) Rich, A.; Crick, F. H. C. *J. Mol. Biol.* **1961**, *3*, 483.
(4) Fraser, R. D. B.; MacRae, T. P.; Suzuki, E. *J. Mol. Biol.* **1979**, *129*, 463.
(5) Li, M. H.; Fan, P.; Brodsky, B.; Baum, J. *Biochemistry* **1993**, *32*, 7377.
(6) Berisio, R.; Vitagliano, L.; Mazzarella, L.; Zagari, A. *Biopolymers* **2001**, *56*, 8.
(7) Berisio, R.; Vitagliano, L.; Mazzarella, L.; Zagari, A. *Protein Sci.* **2002**, *11*, 262.
(8) Okuyama, K.; Hongo, C.; Fukushima, R.; Wu, G.; Narita, H.; Noguchi, K.; Tanaka, Y.; Nishino, N. *Biopolymers* **2004**, *76*, 367.

(9) Momany, F. A.; McGuire, R. F.; Burgess, A. W.; Scheraga, H. A. *J. Phys. Chem.* **1975**, *79*, 2361.
(10) Berg, R. A.; Prockop, D. J. *Biochem. Biophys. Res. Commun.* **1973**, *52*, 115.
(11) Sakakibara, S.; Inouye, K.; Shudo, K.; Kishida, Y.; Kobayashi, Y.; Prockop, D. J. *Biochim. Biophys. Acta* **1973**, *303*, 198.
(12) Holmgren, S. K.; Taylor, K. M.; Bretscher, L. E.; Raines, R. T. *Nature* **1998**, *392*, 666.
(13) Holmgren, S. K.; Bretscher, L. E.; Taylor, K. M.; Raines, R. T. *Chem. Biol.* **1999**, *6*, 63.
(14) Ramachandran, G. N.; Bansal, M.; Bhatnagar, R. S. *Biochim. Biophys. Acta* **1973**, *322*, 166.
(15) Bella, J.; Eaton, M.; Brodsky, B.; Berman, H. M. *Science* **1994**, *266*, 75.
(16) Bella, J.; Brodsky, B.; Berman, H. M. *Structure* **1995**, *3*, 893.
(17) Panasik, N., Jr.; Eberhardt, E. S.; Edison, A. S.; Powell, D. R.; Raines, R. T. *Int. J. Pept. Protein Res.* **1994**, *44*, 262.
(18) Bretscher, L. E.; Jenkins, C. L.; Taylor, K. M.; DeRider, M. L.; Raines, R. T. *J. Am. Chem. Soc.* **2001**, *123*, 777.
(19) DeRider, M. L.; Wilkens, S. J.; Waddell, M. J.; Bretscher, L. E.; Weinhold, F.; Raines, R. T.; Markley, J. L. *J. Am. Chem. Soc.* **2002**, *124*, 2497.
(20) Hinderaker, M. P.; Raines, R. T. *Protein Sci.* **2003**, *12*, 1188.
(21) Improta, R.; Benzi, C.; Barone, V. *J. Am. Chem. Soc.* **2001**, *123*, 12568.
(22) Inouye, K.; Kobayashi, Y.; Kyogoku, Y.; Kishida, Y.; Sakakibara, S.; Prockop, D. J. *Arch. Biochem. Biophys.* **1982**, *219*, 198.
(23) Inouye, K.; Sakakibara, S.; Prockop, D. J. *Biochim. Biophys. Acta* **1976**, *420*, 133.
(24) Vitagliano, L.; Berisio, R.; Mazzarella, L.; Zagari, A. *Biopolymers* **2001**, *58*, 459.
(25) Vitagliano, L.; Berisio, R.; Mastrangelo, A.; Mazzarella, L.; Zagari, A. *Protein Sci.* **2001**, *10*, 2627.
(26) Hodges, J. A.; Raines, R. T. *J. Am. Chem. Soc.* **2003**, *125*, 9262.
(27) Doi, M.; Nishi, Y.; Uchiyama, S.; Nishiuchi, Y.; Nakazawa, T.; Ohkubo, T.; Kobayashi, Y. *J. Am. Chem. Soc.* **2003**, *125*, 9922.
(28) Nishi, Y.; Uchiyama, S.; Doi, M.; Nishiuchi, Y.; Nakazawa, T.; Ohkubo, T.; Kobayashi, Y. *Biochemistry* **2005**, *44*, 6034.
(29) Berisio, R.; Granata, V.; Vitagliano, L.; Zagari, A. *J. Am. Chem. Soc.* **2004**, *126*, 11402.
(30) Mizuno, K.; Hayashi, T.; Peyton, D. H.; Bächinger, H. P. *J. Biol. Chem.* **2004**, *279*, 38072.
(31) Schumacher, M.; Mizuno, K.; Bächinger, H. P. *J. Biol. Chem.* **2005**, *280*, 20397.
(32) Eberhardt, E. S.; Panasik, N., Jr.; Raines, R. T. *J. Am. Chem. Soc.* **1996**, *118*, 12261.
(33) Renner, C.; Alefelder, S.; Bae, J. H.; Budisa, N.; Huber, R.; Moroder, L. *Angew. Chem., Int. Ed.* **2001**, *40*, 923.
(34) Kang, Y. K. *THEOCHEM* **2004**, *675*, 37 and references therein.
(35) Kang, Y. K.; Park, H. S. *Biophys. Chem.* **2005**, *113*, 93 and references therein.
(36) Benzi, C.; Improta, R.; Scalmani, G.; Barone, V. *J. Comput. Chem.* **2002**, *23*, 341.
(37) Rankin, K. N.; Boyd, R. J. *J. Phys. Chem. A* **2002**, *106*, 11168.
(38) Lam, J. S. W.; Koo, J. C. P.; Hudáky, I.; Varro, A.; Papp, J. G.; Penke, B.; Csizmadia, I. G. *THEOCHEM* **2003**, *666*−*667*, 285.
(39) Quan, J.-M.; Wu, Y.-D. *J. Theor. Comput. Chem.* **2004**, *3*, 225.
(40) Song, I. K.; Kang, Y. K. *J. Phys. Chem. B* **2005**, *109*, 16982.
(41) Kang, Y. K. *J. Phys. Chem. B* **2004**, *108*, 5463.
(42) Jhon, J. S.; Kang, Y. K. *J. Phys. Chem. A* **1999**, *103*, 5436.
(43) Frisch, M. J.; Trucks, G. W.; Schlegel, H. B.; Scuseria, G. E.; Robb, M. A.; Cheeseman, J. R.; Zakrzewski, V. G.; Montgomery, J. A., Jr.; Stratmann, R. E.; Burant, J. C.; Dapprich, S.; Millam, J. M.; Daniels, A. D.; Kudin, K. N.; Strain, M. C.; Farkas, O.; Tomasi, J.; Barone, V.; Cossi, M.; Cammi, R.; Mennucci, B.; Pomelli, C.; Adamo, C.; Clifford, S.; Ochterski, J.; Petersson, G. A.; Ayala, P. Y.; Cui, Q.; Morokuma, K.; Malick, D. K.; Rabuck, A. D.; Raghavachari, K.; Foresman, J. B.; Cioslowski, J.; Ortiz, J. V.; Baboul, A. G.; Stefanov, B. B.; Liu, G.; Liashenko, A.; Piskorz, P.; Komaromi, I.; Gomperts, R.; Martin, R. L.; Fox, D. J.; Keith, T.; Al-Laham, M. A.; Peng, C. Y.; Nanayakkara, A.; Gonzalez, C.; Challacombe, M.; Gill, P. M. W.; Johnson, B.; Chen, W.; Wong, M. W.; Andres, J. L.; Gonzalez, C.; Head-Gordon, M.; Replogle, E. S.; Pople, J. A. *Gaussian 98*, revision A.7; Gaussian, Inc.: Pittsburgh, PA, 1998.
(44) Frisch, M. J.; Trucks, G. W.; Schlegel, H. B.; Scuseria, G. E.; Robb, M. A.; Cheeseman, J. R.; Montgomery, J. A., Jr.; Vreven, T.; Kudin, K. N.; Burant, J. C.; Millam, J. M.; Iyengar, S. S.; Tomasi, J.; Barone, V.; Mennucci, B.; Cossi, M.; Scalmani, G.; Rega, N.; Petersson, G. A.; Nakatsuji, H.; Hada, M.; Ehara, M.; Toyota, K.; Fukuda, R.; Hasegawa, J.; Ishida, M.; Nakajima, T.; Honda, Y.; Kitao, O.; Nakai, H.; Klene, M.; Li, X.; Knox, J. E.; Hratchian, H. P.; Cross, J. B.; Adamo, C.; Jaramillo, J.; Gomperts, R.; Stratmann, R. E.; Yazyev, O.; Austin, A. J.; Cammi, R.; Pomelli, C.; Ochterski, J. W.; Ayala, P. Y.; Morokuma, K.; Voth, G. A.; Salvador, P.; Dannenberg, J. J.; Zakrzewski, V. G.; Dapprich, S.; Daniels, A. D.; Strain, M. C.; Farkas, O.; Malick, D. K.; Rabuck, A. D.; Raghavachari, K.; Foresman, J. B.; Ortiz, J. V.; Cui, Q.; Baboul, A. G.; Clifford, S.; Cioslowski, J.; Stefanov, B. B.; Liu, G.; Liashenko, A.; Piskorz, P.; Komaromi, I.; Martin, R. L.; Fox, D. J.; Keith, T.; Al-Laham, M. A.; Peng, C. Y.; Nanayakkara, A.; Challacombe, M.; Gill, P. M. W.; Johnson, B.; Chen, W.; Wong, M. W.; Gonzalez, C.; Pople, J. A. *Gaussian 03*, revision B.01; Gaussian, Inc.: Pittsburgh, PA, 2003.
(45) Némethy, G.; Gibson, K. D.; Palmer, K. A.; Yoon, C. N.; Paterlini, G.; Zagari, A.; Rumsey, S.; Scheraga, H. A. *J. Phys. Chem.* **1992**, *96*, 6472.
(46) Zimmerman, S. S.; Pottle, M. S.; Némethy, G.; Scheraga, H. A. *Macromolecules* **1977**, *10*, 1.
(47) Kang, Y. K. *THEOCHEM* **2001**, *546*, 183.
(48) Császár, A. G.; Perczel, A. *Prog. Biophys. Mol. Biol.* **1999**, *71*, 243.
(49) Czinki, E.; Császár, A. G. *Chem.*−*Eur. J.* **2003**, *9*, 1008.
(50) Wiberg, K. B. *J. Comput. Chem.* **2004**, *25*, 1342.
(51) Barone, V.; Cossi, M. *J. Phys. Chem. A* **1998**, *102*, 1995.
(52) Frisch, A.; Frisch, M. J.; Trucks, G. W. *Gaussian 03 User's Reference*, version 7.0; Gaussian, Inc.: Pittsburgh, PA, 2003.
(53) Kang, Y. K.; Park, H. S. *THEOCHEM* **2004**, *676*, 171.
(54) Takano, Y.; Houk, K. N. *J. Chem. Theory Comput.* **2005**, *1*, 70.
(55) Kang, Y. K.; Park, H. S. *THEOCHEM* **2002**, *593*, 55.
(56) Kang, Y. K.; Choi, H. Y. *Biophys. Chem.* **2004**, *111*, 135.
(57) Kang, Y. K. *J. Phys. Chem. B* **2002**, *106*, 2074.
(58) Kang, Y. K. *THEOCHEM* **2002**, *585*, 209.
(59) Zimmerman, S. S.; Scheraga, H. A. *Macromolecules* **1976**, *9*, 408.
(60) Cremer, D.; Pople, J. A. *J. Am. Chem. Soc.* **1975**, *97*, 1354.
(61) Altona, C.; Sundaralingam, M. *J. Am. Chem. Soc.* **1972**, *94*, 8205.
(62) Han, S. J.; Kang, Y. K. *THEOCHEM* **1996**, *362*, 243.
(63) Fischer, S.; Dunbrack, R. L., Jr.; Karplus, M. *J. Am. Chem. Soc.* **1994**, *116*, 11931.
(64) Matsuzaki, T.; Iitaka, Y. *Acta Crystallogr., Sect. B* **1971**, *27*, 507.
(65) Madison, V.; Schellman, J. *Biopolymers* **1970**, *9*, 511.
(66) Starting from the conformation tCd of Ac-Pro-NHMe optimized at the HF/6-31+G(d) level of theory,[34] we located the local minimum tFd for Ac-Pro-OMe with $\omega' = 177.7°$, $\phi = -70.8°$, $\psi = 156.3°$, $\omega = 179.4°$, $\chi^0 = -15.3°$, $\chi^1 = 31.2°$, $\chi^2 = -35.9°$, $\chi^3 = 26.6$, and $\chi^4 = -7.1°$ at the HF/6-31+G(d) level of theory.
(67) Ramachandran, G. N.; Sasisekharan, V. *Adv. Protein Chem.* **1968**, *23*, 283.
(68) Calculated in this work. See footnote *g* of Tables S1 and S3 of the Supporting Information.
(69) Cox, C.; Lectka, T. *J. Am. Chem. Soc.* **1998**, *120*, 10660.
(70) Harmony, M. D.; Laurie, V. W.; Kuczkowski, R. L.; Schwendeman, R. H.; Ramsay, D. A.; Lovas, F. J.; Lafferty, W. J.; Maki, A. G. *J. Phys. Chem. Ref. Data* **1979**, *8*, 619.
(71) Schultz, G.; Hargittai, I. *J. Phys. Chem.* **1993**, *97*, 4966.
(72) Madison, V.; Kopple, K. D. *J. Am. Chem. Soc.* **1980**, *102*, 4855.
(73) Delaney, N. G.; Madison, V. *J. Am. Chem. Soc.* **1982**, *104*, 6635.
(74) Beausoleil, E.; Lubell, W. D. *J. Am. Chem. Soc.* **1996**, *118*, 12902.
(75) Beausoleil, E.; Sharma, R.; Michnick, S. W.; Lubell, W. D. *J. Org. Chem.* **1998**, *63*, 6572.
(76) Stein, R. L. *Adv. Protein Chem.* **1993**, *44*, 1 and references therein.